Neutron Structure and Inelastic-Neutron-Scattering and Theoretical Studies of $Mo(CO)(H_2)[(C_6D_5)_2PC_2H_4P(C_6D_5)_2]_2 \cdot 4.5C_6D_6$, a Complex with an Extremely Low Barrier to H_2 Rotation. Implications on the Reaction Coordinate for H-H Cleavage to Dihydride

Gregory J. Kubas,*,† Carol J. Burns,† Juergen Eckert,‡ Susanna W. Johnson,‡ Allen C. Larson,‡ Phillip J. Vergamini,‡ Clifford J. Unkefer,† G. R. K. Khalsa,§ Sarah A. Jackson,∥ and Odile Eisenstein∥

Contribution from the Inorganic and Structural Chemistry Group and Manuel Lujan, Jr. Neutron Scattering Center, Los Alamos National Laboratory, Los Alamos, New Mexico 87545, Department of Chemistry, Thiel College, Greenville, Pennsylvania 16125, and Laboratoire de Chimie Théorique, Bâtiment 490, Université de Paris-Sud, 91405 Orsay, France.
Received May 18, 1992

Abstract: The synthesis and characterization of derivatives of $Mo(CO)(R_2PC_2H_4PR_2)_2$ (R = Et, *i*-Bu, Ph, Et-Ph) and their reactions with H_2, N_2, and SO_2 are reported. For R = Et and *i*-Bu, the H_2 oxidatively adds to give dihydrides, but for R = Ph, a η^2-H_2 complex is formed. Electronic considerations, primarily back-bonding to H_2 σ^*, are shown to be the primary cause of H-H bond cleavage. Single-crystal neutron diffraction of $Mo(CO)(H_2)(Ph_2PC_2H_4PPh_2)_2$ (as a 4.5-benzene solvate with all Ph groups deuterated) at 12 K showed the H-H bond to be oriented trans to the CO and parallel to a P-Mo-P axis, with a length close to that of free H_2 (0.74 Å). However, the thermal ellipsoids were very large, and inelastic neutron scattering showed that the barrier to rotation of the H_2 is the lowest yet measured, ca. 0.7 kcal/mol. These observations indicate that librational motion of the H_2 is artificially foreshortening the H-H bond length. Application of a correction procedure gave a distance of 0.80-0.85 Å as being more likely. Extended Huckel calculations successfully modeled the H_2 coordination and also showed a low rotational barrier (1.4 kcal/mol). Theoretical considerations suggest that the degree of distortion of the MP_4 skeleton is largely responsible for the ability of the complex to bind molecular hydrogen and controls the amount of back-bonding from the metal d-orbital to H_2 σ^*. $Mo(CO)(H_2)(Ph_2PC_2H_4PPh_2)_2$ is now the fourth dihydrogen complex to show an H-H neutron distance of ca. 0.82 Å despite widely varying ligand sets, central metals, and charges. The lack of an elongated H-H bond length or equilibrium with a dihydride tautomer, despite the apparent nearness of the H_2 to cleavage, leads to the conclusion that the reaction coordinate for oxidative addition of H_2 is rather flat until relatively precipitous cleavage of the H_2. $Mo(CO)(H_2)[(C_6D_5)_2PC_2H_4P(C_6D_5)_2]_2 \cdot 4.5C_6D_6$ crystallizes in the space group $P\bar{1}$. The cell dimensions (X-ray, 233 K) are as follows: a = 13.038 (3) Å, b = 14.125 (3) Å, c = 19.995 (4) Å, α = 90.42 (3)°, β = 94.48 (3)°, γ = 113.83 (3)°, Z = 2; R = 4.2%.

Introduction

A major goal of our research has been to map the reaction coordinate for hydrogen activation by transition metal centers, focusing upon the structure and dynamics of metal-η^2-H_2 binding. It is now clear from this and extensive other work that H_2 complexes are not merely "arrested intermediates" on the path toward hydride formation but rather have their own unique identity.[1] Although surprisingly similar H-H distances of 0.82 Å have been found in the neutron structures of such diverse species as $W(CO)_3(P\text{-}i\text{-}Pr_3)_2(H_2)$,[2] $FeH(H_2)(dppe)_2^+$,[3] and $FeH_2(H_2)(PPh_2Et)_3$,[4] recent X-ray[5] and NMR[6] studies indicate distances >1 Å exist in other complexes. These studies and neutron data[7] showing an H···H separation of 1.36 Å in $ReH_7[P(p\text{-tolyl})_3]_2$ suggest that a near continuum of distances might be possible, ranging from 0.74 Å (free H_2) to >1.6 Å (hydrides). Also directly relevant to H_2 activation is the existence of dynamic equilibria between dihydrogen and dihydride "tautomers" in $W(CO)_3(PR_3)_2(H_2)$ and several other H_2 complexes.[1,6d,e,8]

Both this behavior and elongated H-H bonds are symptomatic of H_2 approaching complete splitting. The question[8g] then arises as to why some H_2 complexes give equilibria while others appear to manifest extraordinary H-H bond elongation. In cases where

† Inorganic and Structural Chemistry Group (INC-1), MS C346, Los Alamos National Laboratory.
‡ Manuel Lujan, Jr. Neutron Scattering Center (LANSCE), Los Alamos National Laboratory.
§ Thiel College.
∥ Université de Paris-Sud.

(1) Review articles: (a) Kubas, G. J. *Acc. Chem. Res.* **1988**, *21*, 120. (b) Crabtree, R. H. *Acc. Chem. Res.* **1990**, *23*, 95. (c) Ginsburg, A. G.; Bagaturyants, A. A. *Metalloorg. Khim.* **1989**, *2*, 249. (d) Jessop, P. G.; Morris, R. H. *Coord. Chem. Rev.*, in press.
(2) (a) Kubas, G. J.; Ryan, R. R.; Swanson, B. I.; Vergamini, P. J.; Wasserman, H. J. *J. Am. Chem. Soc.* **1984**, *106*, 451. (b) Kubas, G. J.; Unkefer, C. J.; Swanson, B. I.; Fukushima, E. *J. Am. Chem. Soc.* **1986**, *108*, 7000.
(3) Ricci, J. S.; Koetzle, T. F.; Bautista, M. T.; Hofstede, T. M.; Morris, R. H.; Sawyer, J. F. *J. Am. Chem. Soc.* **1989**, *111*, 8823.
(4) Van Der Sluys, L. S.; Eckert, J.; Eisenstein, O.; Hall, J. H.; Huffman, J. C.; Jackson, S. A.; Koetzle, T. F.; Kubas, G. J.; Vergamini, P. J.; Caulton, K. G. *J. Am. Chem. Soc.* **1990**, *112*, 4831.
(5) (a) Kim, Y.; Deng, H.; Meek, D. W.; Wojcicki, A. *J. Am. Chem. Soc.* **1990**, *112*, 2798. (b) Cotton, F. A.; Luck, R. L. *Inorg. Chem.* **1991**, *30*, 767. The H-H distances (1.08 (5) and 1.17 (13) Å) in these Re complexes had the expected large standard deviations.
(6) (a) Hamilton, D. G.; Crabtree, R. H. *J. Am. Chem. Soc.* **1988**, *110*, 4126. (b) Bautista, M. T.; Earl, K. A.; Maltby, P. A.; Morris, R. H.; Schweitzer, C. T.; Sella, A. *J. Am. Chem. Soc.* **1988**, *110*, 7031. (c) Zilm, K. W.; Millar, J. M. *Adv. Magn. Opt. Reson.* **1990**, *15*, 163. (d) Earl, K. A.; Jia, G.; Maltby, P. A.; Morris, R. H. *J. Am. Chem. Soc.* **1991**, *113*, 3027. (e) Jia, G.; Lough, A. J.; Morris, R. H. *Organometallics* **1992**, *11*, 161. (f) Luo, X.-L.; Crabtree, R. H. *J. Chem. Soc., Dalton Trans.* **1991**, 587.
(7) Brammer, L.; Howard, J. A. K.; Johnson, O.; Koetzle, T. F.; Spencer, J. L.; Stringer, A. M. *J. Chem. Soc., Chem. Commun.* **1991**, 241.
(8) (a) Chinn, M. S.; Heinekey, D. M. *J. Am. Chem. Soc.* **1987**, *109*, 5865. (b) Arliguie, T.; Border, C.; Chaudret, B.; Devillers, J.; Poilblanc, R. *Organometallics* **1989**, *8*, 1308. (c) Cotton, F. A.; Luck, R. L. *Inorg. Chem.* **1989**, *28*, 6. (d) Luo, X.-L.; Crabtree, R. H. *J. Am. Chem. Soc.* **1990**, *112*, 6912. (e) Jia, G.; Morris, R. H. *J. Am. Chem. Soc.* **1991**, *113*, 875. (f) Esteruelas, M. A.; Oro, L. A.; Valero, C. *Organometallics* **1991**, *10*, 462. (g) Luo, X.-L.; Michos, D.; Crabtree, R. H. *Organometallics* **1992**, *11*, 237.

0002-7863/93/1515-569$04.00/0

Scheme I

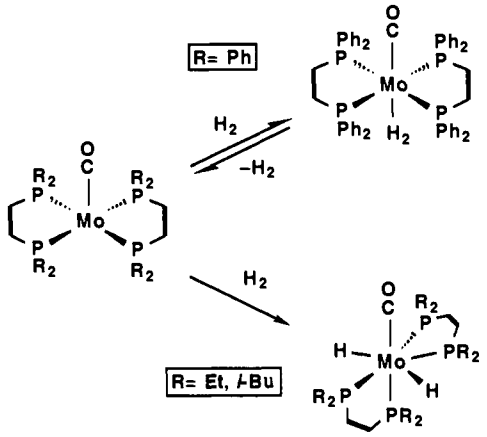

more than two hydrogens surround a metal, delocalized σ-bonding analogous to π-systems such as allyl is a possibility:

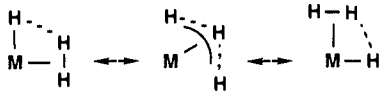

This is supported by the identification of a "cis interaction" between the neighboring M–H σ and H–H σ^* orbitals in $FeH_2(H_2)(PPh_2Et)_3$[4] (as well as other polyhydrides studied theoretically by Eisenstein[9]), long-range interactions between hydrides,[10] and theoretical studies of η^3-H_3 ligands/intermediates.[11] The latter have been fairly well experimentally established to be transients in solution hydride-exchange processes.[8d] It would be tempting to propose that elongated H–H bonds occur only in complexes with >2 metal-bound hydrogens and that η^2-H_2/hydride equilibria correlate with complexes with only two hydrogens (for which bond delocalization cannot occur). While this is generally true, exceptions to both cases are known, in particular $ReCl(H_2)(PPh_2Me)_4$ (H–H = 1.17 (13) Å, X-ray), which may possess an asymmetric or even end-on-bonded H_2.[5b]

In addition to H–H separation, a critical related matter of concern is the extensive motion of hydrogen about the metal, e.g. rotation, which normally is extremely facile even at lower temperatures in the solid state. This can be a factor in both spectroscopic studies and the crystallographic problem of locating hydrogen positions, leading to false or inaccurate information. Quantum-mechanical motion, such as exchange coupling between hydrides,[12] can begin to appear for hydrogen at surprisingly high temperatures (~200 K) and give NMR anomalies. We have been studying classical and quantum-mechanical rotational motion of H_2 by inelastic-neutron-scattering (INS) methods, particularly rotational tunneling spectroscopy.[4,13] As will be demonstrated in this paper, rotation of H_2 about the M–H_2 axis distorts standard crystallographic measurements of H–H distances, even at very low temperatures. On the other hand, *INS detection of rotation is absolutely diagnostic of bound H_2* and gives the rotational energy barrier, a valuable parameter in evaluating metal→H_2 σ^* back-bonding, especially combined with theoretical analysis. The degree of back-donation has been generally believed to directly control H–H bond cleavage. Thus, a challenge remains to determine and correlate structural, dynamic, bonding, and vibrational features of bound H_2, the simplest yet most elusive chemical species.

One strategy to attain this goal is to vary ancillary ligands and hence back-bonding capability of the metal. An excellent system for such a study is based on the 16e complex $Mo(CO)(dppe)_2$[14] (dppe = $Ph_2PC_2H_4PPh_2$) and its congeners, which might be expected to activate H_2 more than $Mo(CO)_3(PR_3)_2(H_2)$ because of the more electron-donating ligand set. The X-ray structure of its reaction product with H_2 has been communicated,[15] and although an η^2-H_2 ligand was not located, spectral properties were compatible with one. A subsequent note[16] showed that merely changing the substituent on the diphosphine from Ph to a more electron-donating alkyl gave a 7-coordinate dihydride instead of the 6-coordinate H_2 complex (Scheme I). This was the first evidence that electronic rather than steric factors (e.g. bulky coligands) are more critical in stabilizing dihydrogen coordination and that increasing M→H_2 σ^* back-bonding leads to H–H bond breaking.

Further details concerning these complexes are presented here, including neutron diffraction, INS, and theoretical studies of $Mo(CO)(H_2)(dppe\text{-}d_{20})_2 \cdot 4.5C_6D_6$. These show that it has the lowest barrier to rotation yet measured for η^2-H_2. As a consequence, the H–H distance determined by least-squares refinement is significantly shorter than the true value. This paper addresses both the reaction coordinate for H_2 cleavage and determination of the H–H distance in a complex wherein H_2 is undergoing extensive librational motion even at 12 K.

Experimental Section

Reactions were carried out under argon and/or H_2 atmospheres using Schlenk techniques. Solvents distilled from Na/K alloy and high-purity argon and/or H_2 were generally used in the syntheses. $Cl_2PC_2H_4PCl_2$ (plus other phosphines) and Ph-d_5-MgBr (0.5 M in THF) were purchased from Strem Chemical and Aldrich Chemical, respectively. Benzyl propionate was obtained from Lancaster Synthesis Inc. or Pfaltz and Bauer and was used as received. $Mo(CO)(dppe)_2$ was prepared by a modification of the literature method[14] (see below). *trans*-$Mo(N_2)_2(dppe)_2$ was synthesized by the literature method,[17] and preparations of the Ph-d_5 and alkyl derivatives were based on it. FT-IR and ^1H NMR spectra were recorded on Bio-Rad FTS-40 and Bruker AM-200 instruments. ^{31}P NMR utilized a 250-MHz IBM instrument and H_3PO_4 reference. Elemental analyses were performed by Galbraith Laboratories, Inc., Knoxville, TN.

Synthesis of $(C_6D_5)_2PC_2H_4P(C_6D_5)_2$ (dppe-d_{20}). A solution of 5.88 mL (10 g, 43 mmol) of $Cl_2PC_2H_4PCl_2$ in 67 mL of Et_2O was added over a 20-min period to 520 mL of Ph-d_5-MgBr (0.5 M in THF, 260 mmol) magnetically stirred in a 1-L flask cooled in an ice bath. The mixture was stirred at room temperature overnight, and 120 mL of toluene was added. A solution of 41.7 g of NH_4Cl in 167 mL of H_2O was *slowly* added with stirring at 0 °C. *Caution:* rapid addition will cause overheating. The mixture was warmed to room temperature, 60 mL of toluene was added, and the organic layer was removed by cannula. The reaction mixture was extracted with additional toluene, and the combined extracts were dried over anhydrous Na_2SO_4 and then decanted (Na_2SO_4 residue was extracted with Et_2O). Solvent was removed in vacuo until the product began to crystallize, whereupon addition of 175 mL of EtOH and further solvent removal for ca. 10 min completed precipitation. The resulting white microcrystalline dppe-d_{20} was dried in vacuo with moderate heating to remove EtOH. The yield was 14.76 g (82%).

Synthesis of $R_2PC_2H_4PR_2$ (R = *i*-Pr, *i*-Bu). The preparations followed literature methods, e.g. those for the R = Et, Cy derivatives.[18] The crude Et_2O solution of *i*-$Pr_2PC_2H_4P$-*i*-Pr_2 was treated with CS_2 to

(9) (a) Jackson, S. A.; Eisenstein, O. *Inorg. Chem.* **1990**, *29*, 3910. (b) Chaudret, B.; Chung, G.; Eisenstein, O.; Jackson, S. A.; Lahoz, F. J.; Lopez, J. A. *J. Am. Chem. Soc.* **1991**, *113*, 2314. (c) Riehl, J.-F.; Pelissier, M.; Eisenstein, O. *Inorg. Chem.* **1992**, *31*, 3344.

(10) Jackson, S. A.; Eisenstein, O. *J. Am. Chem. Soc.* **1990**, *112*, 7203.

(11) (a) Burdett, J. K.; Phillips, J. R.; Pourian, M. R.; Poliakoff, M.; Turner, J. J.; Upmacis, R. *Inorg. Chem.* **1987**, *26*, 3054. (b) Maseras, F.; Duran, M.; Lledos, A.; Bertran, J. *J. Am. Chem. Soc.* **1992**, *114*, 2922.

(12) (a) Zilm, K. W.; Heinekey, D. M.; Millar, J. M.; Payne, N. G.; Demou, P. *J. Am. Chem. Soc.* **1989**, *111*, 3088. (b) Zilm, K. W.; Heinekey, D. M.; Millar, J. M.; Payne, N. G.; Neshyba, S. P.; Duchamp, J. C.; Szczyrba, J. *J. Am. Chem. Soc.* **1990**, *112*, 920. (c) Jones, D.; Labinger, J. A.; Weitekamp, J. *J. Am. Chem. Soc.* **1989**, *111*, 3087. (d) Barthelat, J. C.; Chaudret, B.; Daudey, J. P.; De Loth, Ph.; Poilblanc, R. *J. Am. Chem. Soc.* **1991**, *113*, 9896.

(13) (a) Eckert, J.; Kubas, G. J.; Dianoux, A. J. *J. Chem. Phys.* **1988**, *88*, 466. (b) Eckert, J.; Kubas, G. J.; Hall, J. H.; Hay, P. J.; Boyle, C. M. *J. Am. Chem. Soc.* **1990**, *112*, 2324. (c) Eckert, J.; Blank, H.; Bautista, M. T.; Morris, R. H. *Inorg. Chem.* **1990**, *29*, 747. (d) Eckert, J. *Spectrochim. Acta* **1992**, *48A*, 363. (e) Eckert, J.; Kubas, G. J.; White, R. P. *Inorg. Chem.* **1992**, *31*, 1550.

(14) Sato, M.; Tatsumi, T.; Kodama, T.; Hidai, M.; Uchida, T.; Uchida, Y. *J. Am. Chem. Soc.* **1978**, *100*, 4447.

(15) Kubas, G. J.; Ryan, R. R.; Wrobleski, D. A. *J. Am. Chem. Soc.* **1986**, *108*, 1339.

(16) Kubas, G. J.; Ryan, R. R.; Unkefer, C. J. *J. Am. Chem. Soc.* **1987**, *109*, 8113.

(17) George, T. A.; Noble, M. E. *Inorg. Chem.* **1978**, *17*, 1678.

(18) Burt, R. J.; Chatt, J.; Hussain, W.; Leigh, G. J. *J. Organomet. Chem.* **1979**, *182*, 203.

precipitate the bis-CS_2 adduct in 62% yield (for a 65-mmol scale). The latter was refluxed in 400 mL of EtOH, EtOH–CS_2 being distilled off to leave a yellow liquid residue of the diphosphine. Vacuum distillation was used for the final purification, giving a colorless liquid (bp 120–125 °C at 0.2 Torr). The liquid *i*-Bu analogue was purified directly by vacuum distillation of the crude product, collecting distillate in the boiling range 120–140 °C at 0.1 Torr (74% yield). *Caution*: the diphosphines smoked and nearly inflamed in air.

Synthesis of *trans*-$Mo(N_2)_2$(dppe-d_{20})$_2$. A procedure similar to that for the protio complex[17] was used. $MoCl_5$ (4.03 g, 14.7 mmol) was added portionwise to a solution of dppe-d_{20} (14.76 g, 35.31 mmol) in THF (400 mL) in a 500-mL flask under a *nitrogen* atmosphere (*not* argon or other inert gas!). A 1% Na/Hg amalgam (50 mL of Hg, 6.79 g of Na) was added, and the mixture was stirred for 1 d using a large magnetic stirring bar floating on the amalgam. After solids were allowed to settle undisturbed overnight, the clear orange supernatant was syringed off as well as possible, and the remaining suspension was filtered through Celite (rate is slow). The reaction flask and filter cake were washed with benzene, avoiding amalgam entrainment. The combined solutions of the crude product were stripped to dryness in vacuo, the residue was dissolved in 238 mL of benzene, and the resultant solution was filtered through Celite, the filter cake again being washed with benzene (the filtrate should be carefully checked for the presence of fine particles, which must be removed at this point). The total volume of the solution was now 395 mL, and 634 mL of MeOH was added to precipitate the complex (these exact solvent ratios and *room temperature* crystallization must be used or the MoH_4(dppe-d_{20})$_2$ byproduct will cocrystallize). The yield of orange microcrystals was 7.37 g (51%).

Syntheses of *trans*-$Mo(N_2)_2(R_2PC_2H_4PR_2)_2$ (R = Et, *i*-Pr, *i*-Bu, Et-Ph). These were prepared virtually identically to the Ph-d_5 derivative. For R = Et, the final crystallization utilized 170 mL of benzene and 320 mL of MeOH (5.7 g of $MoCl_5$ as starting material). A 76% yield (8.5 g) of bright orange crystalline product formed (ν(NN) = 1927 cm^{-1}; lit.[17] 1927 cm^{-1}). The yellow-orange *i*-Bu derivative was similarly obtained in 51% yield (ν(NN) = 1947 cm^{-1}).

For R = *i*-Pr, the color of the reaction solution was brownish rather than orange, and the crude product was recrystallized from about half as much solvent, from which a fine orange precipitate formed (ν(NN) = 1918 cm^{-1}). Anal. Calcd for $C_{28}H_{64}N_4P_4Mo$: C, 49.72; H, 9.53; N, 8.28. Found: C, 48.52; H, 9.39; N, 8.02. ^1H NMR (25 °C, benzene-d_6): δ 2.61 (septet, $(CH_3)_2CH$, J = 6.9 Hz), 1.67 (m, PC_2H_4P), 1.40 (m, CH_3).

The mixed alkyl derivative *trans*-$Mo(N_2)_2(Et_2PC_2H_4PPh_2)_2$[19] was also prepared, initially as an oil which solidified on stirring to a deep red-orange powder (ν(NN) = 1940 cm^{-1}; lit.[19] 1945 cm^{-1}).

Synthesis of Mo(CO)(dppe)$_2$ and Mo(CO)(dppe-d_{20})$_2$. The protio and deuterio phosphine complexes were prepared in the same manner, on the basis of substantial modification of the literature procedure.[14] *trans*-$Mo(N_2)_2$(dppe-d_{20})$_2$ (3.77 g, 3.82 mmol) and benzyl propionate (9.1 mL, 9.3 g, 57 mmol) were refluxed in toluene (113 mL) under a slow argon flow through the flask (250 mL, with side arm) and out the condenser to remove displaced N_2. The latter would otherwise recoordinate to the unsaturated product. The solution darkened within minutes, and after a total reflux time of 20 min, the solution volume was slowly reduced in vacuo to ca. 80 mL. The flask was placed in a refrigerator overnight, and the resultant precipitate was filtered off, washed with 1:1 toluene/hexane, and dried in vacuo. The yield of sparingly-soluble black microcrystals of Mo(CO)(dppe-d_{20})$_2$ was 1.96 g (56%).

Synthesis of Mo(CO)(H_2)(dppe)$_2$·3C_6H_6 and Mo(CO)(H_2)(dppe)$_2$·2C_7H_8 Solvates and Isotopomers. A slurry of Mo(CO)(dppe)$_2$ in benzene or toluene (ca. 3 g/15 mL) was stirred for several hours under H_2. The solution became orange, and precipitation occurred (supersaturation may occur if stirring is terminated), which was completed by addition of 20 mL of hexane and further stirring for 1 h. The bright orange microcrystalline product was collected on a frit in nearly quantitative yield and dried in a stream of H_2 and briefly in vacuo. The D_2 and HD complexes were prepared similarly, as well as the deuterio phosphine analogues. The sparingly-soluble complexes were stored and manipulated under H_2 or H_2/argon mixtures. ^1H NMR of Mo(CO)(H_2)(dppe)$_2$ in toluene-d_8 at 300 MHz: δ 6.89–7.50 (m, Ph), 2.22 (m, CH_2), −4.70 (br s, H_2).

Preparation of Mo(CO)(H_2)(dppe-d_{20})$_2$·4.5C_6D_6 and Crystals for Neutron Structure. Well-formed large orange crystals of the H_2 complex as the 4.5C_6D_6 solvate were obtained by reacting H_2 with a slurry of Mo(CO)(dppe-d_{20})$_2$ in benzene-d_6 (ca. 2 g/15 mL) at ~45 °C. Stirring was discontinued when a homogeneous orange solution formed in order to take advantage of supersaturation. The solution was cooled to 30–35 °C, seeded with microcrystalline H_2 complex, and allowed to stand at room temperature under H_2. Within 1 or 2 d, a copious yield of crystals formed, which were collected on a frit, washed with a small amount of benzene-d_6, and carefully dried to avoid loss of H_2 and lattice solvent. The crystals were stored under H_2 in a tube to which a few microliters of benzene-d_6 was added to prevent efflorescence.

Synthesis of Mo(CO)(depe)$_2$ and Mo(CO)(*i*-$Bu_2PC_2H_4P$-*i*-Bu_2)$_2$. $Mo(N_2)_2$(depe)$_2$ (0.81 g, 1.43 mmol), toluene (18 mL), and ethyl acetate (1.3 mL) were refluxed under argon for 40 min as for the preparation of the dppe complex. The solution turned blue-purple but then became bright red-orange on cooling. Partial solvent removal to ca. 3 mL followed by addition of 8 mL of nonane gave a small amount of solid, and further solvent removal to 5 mL produced red-orange microcrystals of Mo(CO)(depe)$_2$. Cooling in a freezer for 2 h, filtration, and washing with 2–3 mL of hexane gave a yield of 0.4 g (52%). The *i*-Bu derivative was prepared in similar fashion, although here the solution turned red-brown instead of purple and did not change on cooling. The complex was again very soluble (even in alkanes) but did crystallize as red-brown prisms on removal of most of the solvent. *Attempts to scale up the above reactions by a factor of 5 were unsuccessful* due to incomplete reactions even after 2.5 h. The *i*-Pr and $Et_2PC_2H_4PPh_2$ derivatives of the N_2 complexes also gave brown-purple solutions on reflux with ester, but no attempts were made to isolate the unsaturated complexes.

Synthesis of MoH_2(CO)(depe)$_2$ and MoH_2(CO)(*i*-$Bu_2PC_2H_4P$-*i*-Bu_2)$_2$. Mo(CO)(depe)$_2$ (0.3 g) in 2–3 mL of hexane was reacted with H_2 to give a yellow solution. Partial solvent removal in vacuo gave some darkening of color toward orange, but readdition of H_2 restored the light yellow color. A nearly colorless crystalline mass of the dihydride suddenly formed on cooling, which redissolved on warming, indicating highly temperature-dependent solubility. Complete solvent removal gave a dry, loose, aggregate mass of elongated crystals of various sizes, which were yellow-tinged on the surface but essentially colorless. The crystals became somewhat more yellow on exposure to vacuum but lightened under H_2. Exposure to air caused surface discoloration to yellow-orange within seconds. Anal. Calcd for $C_{21}H_{50}OP_4Mo$: C, 46.84; H, 9.34. Found: C, 46.47; H, 9.21. ^1H NMR (25 °C, toluene-d_8): δ 1.46 (m, CH_2), 0.97 (m, CH_3), −5.40 (q, MoH_2).

The preparation and properties of colorless platelike crystals of the *i*-Bu analogue were similar. ^1H NMR (25 °C, toluene-d_8): δ 2.22 (broad septet, $(CH_3)_2CH$), 1.68 (m, PCH_2), 1.03 (s, CH_3), 0.97 (s, CH_3), −5.11 (quint, MoH_2).

Synthesis of MoH_2(CO)$(Et_2PC_2H_4PPh_2)_2$. This complex was prepared as those above except that the intermediate unsaturated species was not isolated. H_2 was added directly to the crude solution of Mo(CO)$(N_2)(Et_2PC_2H_4PPh_2)_2$ formed from reflux of the *trans*-$(N_2)_2$ complex under N_2. Partial removal of solvent and MeOH addition under an H_2 atmosphere gave an oily precipitate which crystallized in 1 d to a yellow microcrystalline solid. The complex was not as air-sensitive as the above but did lose H_2 in solution in vacuo. Attempts to prepare the *i*-$Pr_2PC_2H_4P$-*i*-Pr_2 analogue by this method failed.

Preparation of Mo(CO)$(N_2)(R_2PC_2H_4PR_2)_2$ (R = Et, *i*-Bu, Et-Ph). Reflux of reaction mixtures similar to those for the synthesis of Mo(CO)(depe)$_2$, under N_2 instead of argon, gave the N_2 complexes on partial solvent removal and alkane addition. Benzyl propionate or ethyl acetate can be used as the CO source. For R = Et, the product was orange and very soluble (moderately soluble in hexane). For R = *i*-Bu, bright yellow well-formed crystals formed directly upon solvent removal from the toluene reaction mixture and readdition of N_2 (some N_2 was lost on pumping). The complex was quite soluble in alkanes, more so than in acetone or MeOH. Exposure of a nonane solution to vacuum gave a red-brown color, presumably due to the unsaturated species.

Red Mo(CO)$(N_2)(Et_2PC_2H_4PPh_2)_2$ slowly (days) crystallized from the crude reaction mixture after addition of MeOH (ethyl acetate reactant). Attempts to prepare the R = *i*-Pr analogue failed. Only colorless crystals showing no ν(NN) in the IR formed.

H_2/D_2 Exchange Experiments. Finely-divided solid samples of complexes were placed in 15–25-mL flasks and thoroughly dried on a vacuum line for several hours with occasional heating to ~50 °C. H_2 and D_2 (0.5 atm each) were added (measured manometrically), the flask was closed off, and Al foil was placed around it to prevent photolytic reactions. After 9 d, gas samples were analyzed mass spectroscopically. For 0.6 mmol of gas over 0.46 mmol of Mo(CO)(dppe)$_2$, a mixture of 31% H_2, 50% HD, and 19% D_2 was formed. The reason for the presence of more H than D atoms was not clear, although a sample of 0.6 mmol of gas over $Mo(CO)_3(PCy_3)_2$ (0.089 mmol) did give nearly statistical scrambling (24% H_2, 51% HD, 25% D_2). Other samples included 0.8 mmol of gas over Mo(CO)(depe)$_2$ (0.22 mmol), giving 32% H_2, 29% HD, and 37% D_2, and $[FeH(H_2)(dppe)_2]BF_4$ (0.16 mmol), which gave only 7% HD.

Parahydrogen-Induced Polarization (PHIP) Experiments. Para-H_2 was produced by cooling 250-mL flasks filled with H_2 at ambient pressure to liquid nitrogen temperatures for 3–4 h over a catalyst of Fe_2O_3,

(19) Jiabi, C.; Guixin, L.; Xiyan, L. *Kexue Tongbao (Foreign Lang. Ed.)* **1980**, *25*, 919.

Table I. Crystallographic Parameters for $Mo[(C_6D_5)_2PCH_2CH_2P(C_6D_5)_2]_2(CO)(H_2)\cdot 4.5C_6D_6$

	X-ray	neutron
temp, K	233	12
space group	$P\bar{1}$	$P\bar{1}$
a, Å	13.038 (3)	12.9719 (15)
b, Å	14.125 (3)	14.0358 (16)
c, Å	19.995 (4)	19.8364 (16)
α, deg	90.42 (3)	90.533 (8)
β, deg	94.48 (3)	94.390 (7)
γ, deg	113.83 (3)	114.032 (8)
V, Å^3	3355.1 (12)	3285.6
Z	2	2
fw	1341.37	1341.37
ρ_{calcd}, g cm^{-3}	1.327	1.355
μ, cm^{-1}	3.27	0.12 + 0.13λ
crystal size, mm	0.12 × 0.22 × 0.30	3.0 × 3.5 × 2.5
radiation	Mo Kα (λ = 0.71069 Å)	0.5–5.5 Å, variable
scan type, range	θ–2θ, $2 < 2\theta < 45°$	time-of-flight, $0.75 < d < 6.5$ Å
scan speed, deg/min	1.30–16.48, variable	
scan width, deg	0.8 + 0.35 tan θ	
no. of reflns collected	9168 (+h,+k,±l)	23 201
no. of reflns used	6838 ($F_o > 2.5\sigma(F_o)$)	13 238 ($I > 3\sigma(I)$)
no. of variables	775	1502
$R(F)$	0.042	0.094
$R_w(F)$	0.059	0.079
GOF	1.95	
χ^2		13.359

silica gel, and activated carbon. Addition to freeze–thaw degassed NMR samples was performed on a vacuum line. The NMR tubes were thawed, shaken, and placed in the NMR probe (preshimmed). An initial spectrum could be recorded within 30 s. As a "standard", addition of para-H_2 to $IrCl(CO)(PPh_3)_2$ in C_6D_6 was examined, and the PHIP phenomenon was found to occur (~15-min duration) in the ^1H NMR hydride signals of the $IrH_2Cl(CO)(PPh_3)_2$ product as described by Eisenberg.[20] The following complexes were examined similarly (para-H_2 addition to): $W(CO)_2(PR_3)_2$ (R = i-Pr, Cy), $Mo(CO)(dppe)_2$, and $Mo(CO)(i\text{-}Bu_2PC_2H_4P\text{-}i\text{-}Bu_2)_2$. No PHIP effect was observed for any of these samples.

Structural Determination (X-ray). Crystallographic data are summarized in Table I. A single crystal measuring 0.21 × 0.31 × 0.45 mm was mounted in a glass capillary, which was flame-sealed and cooled to 233 K in the cold stream of an Enraf-Nonius CAD4 automated diffractometer. Accurate cell constants and the orientation matrix were determined by a least-squares fit to the setting angles of the unresolved Mo Kα components of 25 reflections with $12° < 2\theta < 30°$. Data were collected utilizing Mo Kα radiation (λ = 0.71069 Å). Examination of the data revealed no systematic absences; the centric triclinic space group $P\bar{1}$ was chosen and the choice confirmed by subsequent refinement. After reduction of the data and correction for Lorentz and polarization effects, the structure was solved by a combination of Patterson and difference Fourier methods. All calculations were carried out utilizing the commercial software package SHELXTL-Plus, and an empirical absorption correction was applied on the basis of the differences between observed and calculated structure factors for the isotropic structure.[21] All nonhydrogen atoms were refined anisotropically. Subsequent difference Fourier maps located most of the hydrogen atoms on the phosphine ligands and the solvate molecules; these were placed in idealized positions but not refined. The maximum peak in the final difference Fourier map was 0.90 e/Å^3 and was located near the molybdenum atom. The function minimized was $\sum w(|F_o| - |F_c|)^2$, with $w^{-1} = \sigma^2(F) + 0.0005F^2$. The final refinement converged (mean $\Delta/\sigma = 0.2$) for 6838 ($F/\sigma(F) > 2.5$) parameters and 776 variables with weighted and unweighted residuals of 0.0592 and 0.0421, with a reduced GOF of 1.95. The dihydrogen ligand could not be located in the final difference Fourier map. Positional and equivalent thermal parameters and anisotropic thermal parameter values are given in supplementary Tables S1 and S3. Table II presents selected bond distances and angles.

Structural Determination (Neutron). Crystallographic data are summarized in Table I. A single-crystal sample measuring 3.0 × 3.5 × 2.5 mm was sealed in a quartz capillary tube under a hydrogen atmosphere. The capillary was glued to the end of a hollow aluminum pin, mounted on the cold finger of a closed-cycle Displex refrigerator, and cooled to a temperature of 12 ± 1 K. The single-crystal neutron data were collected at the Manuel Lujan, Jr. Neutron Scattering Center (LANSCE) on the LANSCE single-crystal diffractometer.[22] This instrument uses Laue geometry to collect the intensity data in a 25 cm × 25 cm ^{3}He-filled two-dimensional position-sensitive proportional counter, covering a 64 × 64 channel array, placed approximately 26 cm from the sample at 2θ =

Table II. Selected Bond Distances and Angles for $Mo[(C_6D_5)_2PCH_2CH_2P(C_6D_5)_2]_2(CO)(H_2)\cdot 4.5C_6D_6$

	X-ray	neutron
Mo–P(1)	2.423 (1)	2.419 (8)
Mo–P(2)	2.447 (2)	2.441 (9)
Mo–P(3)	2.439 (2)	2.442 (8)
Mo–P(4)	2.442 (1)	2.440 (9)
Mo–C(1)	1.933 (5)	1.946 (12)
Mo–H(9)		1.920 (15)
Mo–H(10)		1.924 (15)
Mo–H_2(midpoint)		1.886
H(9)–H(10)		0.736 (10)[a]
P(1)–C(2)	1.860 (5)	1.851 (8)
P(1)–C(6)	1.858 (4)	1.854 (14)
P(1)–C(12)	1.833 (6)	1.826 (7)
P(2)–C(3)	1.867 (5)	1.861 (7)
P(2)–C(18)	1.841 (4)	1.841 (11)
P(2)–C(24)	1.843 (6)	1.842 (6)
P(3)–C(4)	1.870 (5)	1.856 (6)
P(3)–C(30)	1.844 (4)	1.838 (13)
P(3)–C(36)	1.834 (6)	1.844 (6)
P(4)–C(5)	1.851 (6)	1.864 (8)
P(4)–C(42)	1.849 (5)	1.847 (9)
P(4)–C(48)	1.837 (4)	1.826 (12)
C(1)–O(1)	1.179 (6)	1.168 (9)
P(1)–Mo–P(2)	80.6 (1)	80.85 (29)
P(1)–Mo–P(3)	97.5 (1)	97.13 (30)
P(1)–Mo–P(4)	174.2 (1)	173.69 (20)
P(1)–Mo–C(1)	86.1 (1)	85.6 (6)
P(1)–Mo–H_2(midpoint)		93.9
P(2)–Mo–P(3)	170.6 (1)	170.67 (22)
P(2)–Mo–P(4)	102.4 (1)	102.48 (30)
P(2)–Mo–C(1)	91.6 (2)	90.9 (4)
P(2)–Mo–H_2(midpoint)		86.0
P(3)–Mo–P(4)	80.3 (1)	80.43 (30)
P(3)–Mo–C(1)	97.5 (2)	98.0 (4)
P(3)–Mo–H_2(midpoint)		85.0
P(4)–Mo–C(1)	88.8 (1)	89.0 (6)
P(4)–Mo–H_2(midpoint)		91.7
C(1)–Mo–H_2(midpoint)		176.9
Mo–C(1)–O(1)	177.0 (5)	176.6 (4)
Mo–P(1)–C(2)	107.2 (2)	107.16 (31)
Mo–P(1)–C(6)	123.8 (2)	124.1 (5)
Mo–P(1)–C(12)	121.6 (1)	121.6 (4)
C(2)–P(1)–C(6)	99.0 (2)	99.0 (4)
C(2)–P(1)–C(12)	101.3 (2)	100.6 (5)
C(6)–P(1)–C(12)	99.8 (2)	99.9 (4)
Mo–P(2)–C(3)	108.8 (2)	109.4 (3)
Mo–P(2)–C(18)	124.8 (2)	124.8 (4)
Mo–P(2)–C(24)	117.9 (2)	117.7 (5)
C(3)–P(2)–C(18)	100.7 (2)	99.9 (6)
C(3)–P(2)–C(24)	101.4 (2)	101.4 (5)
C(18)–P(2)–C(24)	100.0 (2)	100.1 (5)
Mo–P(3)–C(4)	110.1 (2)	110.4 (4)
Mo–P(3)–C(30)	115.2 (2)	114.8 (4)
Mo–P(3)–C(36)	124.5 (2)	124.1 (5)
C(4)–P(3)–C(30)	101.6 (2)	102.1 (6)
C(4)–P(3)–C(36)	100.3 (2)	100.1 (5)
C(30)–P(3)–C(36)	102.0 (2)	102.3 (4)
Mo–P(4)–C(5)	108.0 (2)	108.1 (3)
Mo–P(4)–C(42)	120.2 (1)	119.1 (5)
Mo–P(4)–C(48)	122.8 (2)	123.5 (5)
C(5)–P(4)–C(42)	102.0 (2)	102.0 (4)
C(5)–P(4)–C(48)	99.9 (2)	99.7 (4)
C(42)–P(4)–C(48)	100.5 (2)	101.0 (5)

[a] The "true" bond length is longer than this, estimated to be 0.80–0.85 Å (see text).

(20) Eisenberg, R. *Acc. Chem. Res.* **1991**, *24*, 110.
(21) (a) *SHELXTL-Plus*; Siemens Analytical X-Ray Corp.: Madison, WI, 1988. (b) Walker, N.; Stuart, D. *Acta Crystallogr.* **1983**, *A39*, 159.
(22) Alkire, R.; Larson, A. C.; Vergamini, P. J. *Acta Crystallogr.* **1985**, *C41*, 1709.

Table III. IR and ^1H NMR Data for $MoH_2(CO)(R_2PC_2H_4PR_2)_2$

compound	color	ν(CO)[a]	ν(HH) or ν(MoH)	$\nu_s(MoH_2)$ or δ(MoH)	δ, Hz[b]	J(HD), Hz	T_1, ms[c]
$Mo(CO)(H_2)(dppe)_2 \cdot xC_6H_6$[d]	orange	1815	2650[e]	875[f]			
$Mo(CO)(H_2)(dppe)_2 \cdot 2C_7H_8$	orange	1814	2650[e]	875[f]	−4.7 s, br	34	20
$Mo(CO)(D_2)(dppe)_2 \cdot 2C_7H_8$	orange	1813		~640[g]			
$MoH_2(CO)(depe)_2$	pale yellow	1790	1647[h]	~715[i]	−5.40 q[j]	<2	370[k]
$MoD_2(CO)(depe)_2$	pale yellow	1790	1194[l]	528[m]			
$MoH_2(CO)(i\text{-}Bu_2PC_2H_4P\text{-}i\text{-}Bu_2)_2$	pale yellow	1780	1658[h]		−5.11 q[j]	<2	200
$MoH_2(CO)(Ph_2PC_2H_4PEt_2)_2$	yellow	1788	1644[h]		−4.3 s, br		

[a] In hexane, except for dppe complexes (Nujol mull). The alkyl derivatives were partially soluble in Nujol. [b] In toluene-d_8. [c] 200 MHz, −70 °C, toluene-d_8. [d] x = 3, 4.5. [e] ν(HH). [f] $\nu_s(MoH_2)$. [g] $\nu_s(MoD_2)$. [h] ν(MoH). [i] δ(MoH). [j] J(PH) = 34 Hz. [k] 1 s at 25 °C. [l] ν(MoD). [m] δ(MoD).

Table IV. IR Data for $Mo(CO)(R_2PC_2H_4PR_2)_2$ and $Mo(CO)(L)(R_2PC_2H_4PR_2)_2$

			ν(CO), cm^{-1}		ν(NN), cm^{-1}	
L	R	color	Nujol	soln	Nujol	soln
	Ph	brown-black	1723			
	Et	red		1748[a]		
	i-Bu	red-brown	1725	1743[a]		
N_2	Ph	yellow-orange	1809		2090	
N_2	Ph-Et	red-orange	1782	1795[b]	2060	2092[b]
N_2	Et	yellow-orange	1776	1796[b]	2050	2070[b]
N_2	i-Bu	yellow		1797[b]		2060[b]

[a] Nujol was the solvent (complex partially dissolves in Nujol mulls). [b] In nonane.

90°, above the horizontal plane. The instrument dimensions were calibrated by refining diffraction data from a 3-mm-diameter spherical Al_2O_3 single crystal (a = 4.766 Å, c = 12.996 Å). The spectral distribution of the source was measured from the incoherent scattering of a 2-mm-diameter bead of $V_{0.95}Nb_{0.05}$. Individual data sets, or histograms, were obtained by holding the sample in a fixed position and measuring the wavelengths of the neutrons in each channel using the Laue time-of-flight technique. The ϕ and ω angles of the diffractometer were adjusted in order to change the crystal orientation and thus cover the hemisphere of reciprocal space required.

Diffraction data were collected in the wavelength range 0.5–5.5 Å. Thirty-four histograms were collected and searched for diffraction maxima, locating 23 201 reflections. Data reduction and least-squares refinement of the structure were performed at LANSCE with the General Structure Analysis System (GSAS).[23] The 60 most intense peaks were used to refine the lattice constants, crystal locations, and crystal orientation angles. The final values of the lattice constants are given in Table I. The intensity data were obtained by integration over a small region at each reflection position, using locations calculated from the lattice constants and crystal orientation and location parameters for each of the 34 crystal settings. The integration was limited to reflections with d spacings greater than 0.75 Å. The intensity data were corrected for the spectral source distribution, the path length of the scattered n. A spherical absorption correction was applied (μ (cm^{-1}) = 0.12 + 0.13λ, T_{min}/T_{max} = 0.87). After the histogram scale factors and extinction parameters were allowed to refine, the known molybdenum, phosphorus, and carbon atom positions were entered with isotropic thermal parameters. All hydrogen and deuterium atom positions were obtained from difference Fourier maps. All atoms were refined anisotropically. Neutron absorption coefficients were obtained from Koster and Yelon[24] for the heavy elements and from Howard, Johnson, Schultz, and Stringer[25] for hydrogen. The function minimized was $\chi^2 = w(F_o - F_c)^2$, with weights determined by $w = (2F_o/\sigma(F_o^2))^2$; $\sigma(F_o^2)$ was based on counting statistics. The neutron scattering lengths[24] used were b_{Mo} = 0.695, b_P = 0.513, b_O = 0.581, b_C = 0.665, b_H = −0.374, and b_D = 0.667. The final refinement converged (all Δ/σ = 0.00) for 13 238 ($I/\sigma(I) > 3$) parameters and 1502 variables with weighted and unweighted residuals of 0.079 and 0.094 and a reduced χ^2 of 13.349. The variable list included 34 scale factors (one for each histogram), 1467 atomic parameters, and a type II[26] extinction coefficient which refined to 3.654×10^{-5}. Final atomic positions and equivalent isotropic thermal parameters and anisotropic thermal parameter values are given in supplementary Tables S2 and S4. Table II presents selected bond distances and angles.

(23) Larson, A. C.; Von Dreele, R. B. Report LAUR 86-748; Los Alamos National Laboratory: Los Alamos, NM, 1986.
(24) Koster, L.; Yelon, W. B. *Neutron Diffraction Newsletter*; Department of Physics, Netherlands Energy Research Foundation: P.O. Box 1, 1755 ZG Petten, The Netherlands, 1982.
(25) Howard, J. A. K.; Johnson, O.; Schultz, A. J.; Stringer, A. M. *J. Appl. Crystallogr.* **1987**, *20*, 120.
(26) (a) Zachariasen, W. H. *Acta Crystallogr.* **1967**, *23*, 558. (b) Larson, A. C. *Acta Crystallogr.* **1967**, *23*, 664.

Results

Synthesis and Characterization of $Mo(CO)(R_2PC_2H_4PR_2)_2$ and Reactions with H_2 and Other Small Molecules. Synthesis of the 16e precursors $Mo(CO)(R_2PC_2H_4PR_2)_2$ was based on extensive modification of the procedure for the complex with R = Ph (dppe),[14] which had been shown by X-ray crystallography to possess a weak agostic interaction of a phenyl hydrogen (Mo···H, 2.95 Å). The original method was a multistep process, the first being preparation of *trans*-$Mo(N_2)_2(dppe)_2$ (eq 1). We prepared

$$MoCl_5 + 2R_2PC_2H_4PR_2 \xrightarrow[THF,\ N_2]{Na/Hg} \textit{trans}\text{-}Mo(N_2)_2(R_2PC_2H_4PR_2)_2 \quad (1)$$

both the known congeners [R = Ph, Et (depe), Ph-Et ($Et_2PC_2H_4PPh_2$)] and also the R = *i*-Pr and *i*-Bu analogues. The next step involved carbonylation of the N_2 complex in refluxing benzene under an N_2 atmosphere, using either DMF or an ester (benzyl propionate) as the stoichiometric CO source, to give *trans*-$Mo(CO)(N_2)(dppe)_2$. The final step was removal of the labile N_2 by passing argon through a benzene solution at 50 °C to give $Mo(CO)(dppe)_2$ (27% overall yield). However, we found the preparation to be inconvenient for multigram quantities because of the low solubilities of the complexes and sought to modify it. The obvious simplification was to combine the last two steps by carrying out the carbonylation under *argon* rather than N_2, and this gave excellent results (eq 2). The reaction solutions

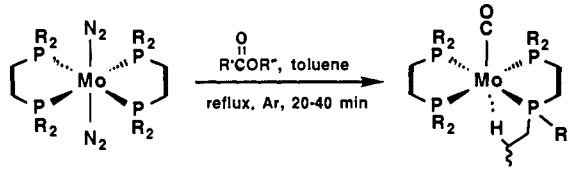

R= Ph, Et, *i*-Bu 50–60% (2)

generally became deep brown (Ph) or purple within minutes. Cooling and partial solvent removal afforded 50–60% yields of crystalline $Mo(CO)(R_2PC_2H_4PR_2)_2$ (R = Ph, Et, *i*-Bu) in excellent purity (infrared CO stretches are given in Table III). Ethyl acetate instead of nonvolatile benzyl propionate was used for preparations of the R = alkyl complexes because their high solubility required nearly complete vacuum removal of liquids. Curiously, the color of the reaction solution for the alkyl derivatives changed from purple to red (the color of the isolated solid) on cooling. It is probable that agostic-type interactions are present for these alkyl derivatives as was found for the phenyl congener,[14] and some form of conformational isomerism or solvent interaction may explain the color differences. For R = Et, attempts to scale up eq 2 to a larger than 1-g preparation led to incomplete reaction. Although purple-brown solutions formed for R = *i*-Pr or Ph-Et, attempts to isolate the unsaturated complexes were not made, and the solutions were used for in situ reactions.

Addition of either H_2 or N_2 to these deeply colored brown or red 16e complexes in hydrocarbon solutions readily gave adducts ranging in color from orange to pale yellow (for R = *i*-Pr, addition to solutions formed in situ according to eq 2 gave only an un-

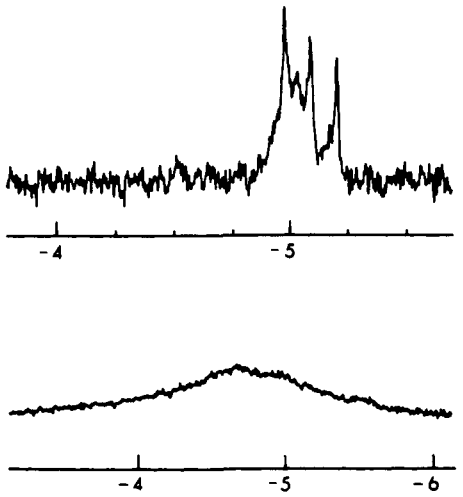

Figure 1. ^{1}H NMR spectra (300 MHz, toluene-d_8, 25 °C) of Mo(CO)(HD)(dppe)$_2$ (upper) and Mo(CO)(H$_2$)(dppe)$_2$ (lower).

characterized colorless product showing no ν(CO) or ν(NN)). The R = Ph complexes are generally sparingly soluble in toluene, but those for R = alkyl are exceedingly soluble, even in hexane. Other properties are summarized in Tables III and IV. The adducts for R = Ph and L = H_2, N_2 gave ^{31}P NMR spectra in benzene-d_6 compatible with octahedral coordination geometry with trans CO and L, i.e. equivalent phosphorus atoms displaying single resonances at δ 73.67 (L = H_2) and 68.28 (L = N_2). As for the dihydrogen complex Mo(CO)$_3$(PR$_3$)$_2$(H$_2$), the product of H_2 addition, Mo(CO)(H$_2$)(dppe)$_2$, is air-sensitive, decomposes in halogenated solvents, and undergoes displacement of H_2 by donor solvents/reactants such as MeCN, pyridine, and SO_2. Large well-formed crystals containing varying amounts of lattice solvent were readily grown by exposing slurries of Mo(CO)(dppe)$_2$ in benzene or toluene to H_2 and allowing the resulting supersaturated solutions to stand undisturbed at ambient temperature. These as well as crystals of a complex with deuterated phenyls, Mo(CO)(H$_2$)[(C$_6$D$_5$)$_2$PC$_2$H$_4$P(C$_6$D$_5$)$_2$]$_2$·4.5C$_6$D$_6$, were used for the extensive X-ray and neutron studies below.

The binding of N_2 is completely reversible, but for the complexes formed from H_2 addition, the ease of extrusion of H_2 under vacuum in solution varies with R in the order Ph > *i*-Bu > Et. Judging by the striking color changes, loss and readdition of H_2 was rapid for the Ph and *i*-Bu species but slow for the Et complex. As will be shown by the spectroscopic data and X-ray and neutron structures below, *the Ph congener indeed contains a dihydrogen ligand but the Et species is a 7-coordinate dihydride* (Scheme I). The structure of the *i*-Bu derivative has not been unequivocally established, although similarity of its IR and NMR spectra to those of the Et species (see below) indicates that it is most probably also a dihydride.

In line with its expected lability, the H_2 ligand in Mo(CO)(H$_2$)(dppe)$_2$ is displaced by N_2, and ^{31}P NMR showed that the trans stereochemistry is retained. SO_2 displaces both bound H_2 and N_2 to give a yellow precipitate. However, ^{31}P NMR of the in situ reaction product of N_2 displacement showed several signals, indicative of formation of isomers/products other than *trans*-Mo(CO)(SO$_2$)(dppe)$_2$. Analogous reaction of SO_2 with MoH$_2$(CO)(depe)$_2$ gives an oily, unstable, reddish material, which is unlike the green-yellow solid obtained by displacement of N_2 from Mo(CO)(N$_2$)(depe)$_2$. It is possible that SO_2 inserts into and/or is reduced by the Mo–H bonds in the dihydride. The SO_2 displacement products were not characterized other than by IR, which showed bands typical of coplanar S-bound SO_2.

IR and ^{1}H NMR Studies of MoH$_2$(CO)(R$_2$PC$_2$H$_4$PR$_2$)$_2$ and Para-H$_2$ Addition Products. For the product of H_2 addition to Mo(CO)(dppe)$_2$, IR and ^{1}H NMR data clearly showed that dihydrogen binding was present. A very broad resonance (Figure 1) was observed for the η^2-H_2 at −4.7 ppm (25 °C, 300 MHz, toluene-d_8). Even at low temperatures, this signal remained broad, and there was no *observable* evidence for the presence of a dihydride tautomer as seen for W(CO)$_3$(PR$_3$)$_2$(H$_2$). The T_1 was measured to be 20 ms at −70 °C and 200 MHz, and J(HD) was determined to be 34 Hz in toluene-d_8 (25 °C) for the complex prepared from HD. Compared to the signal for η^2-H_2 in the spectrum of the perprotio complex, there was a relatively large shift in the position of the 1:1:1 triplet signal for the η^2-HD complex (−5.09 ppm) (Figure 1). The triplet did not shift significantly with field or temperature. The line widths were much narrower for the HD species, which was not unexpected, although the difference in widths is unusually large. Perhaps a factor here is the extremely low rotational barrier for the η^2-H_2 in this complex (see below).

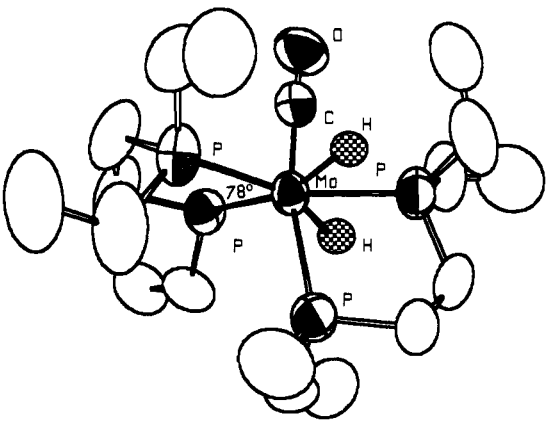

Figure 2. ORTEP drawing of MoH$_2$(CO)(depe)$_2$, with unlocated hydrides placed in idealized positions in the pentagonal plane.

Addition of para-H_2 to Mo(CO)(dppe)$_2$ was also carried out in order to determine if parahydrogen-induced polarization (PHIP)[20] was observable in the ^{1}H NMR of Mo(CO)(H$_2$)(dppe)$_2$. No effect was seen either for this compound or for the related W(CO)$_3$(PR$_3$)$_2$(H$_2$) species. This was not unexpected because oxidative addition–reductive elimination is known to equilibrate ortho and para forms of H_2, and rapid equilibrium with a small amount of dihydride tautomer would probably be enough to eliminate or shorten the effect.

Infrared bands observed for Nujol mulls of the various solvates of Mo(CO)(H$_2$)(dppe)$_2$ included a weak, broad H–H stretch at about 2650 cm^{-1} and partially-obscured underlying features at ca. 875 cm^{-1} (symmetric Mo–H_2 stretch) and ca. 400 cm^{-1} (Mo–H_2 deformational mode). These were shifted in the D_2 complex, which did not show a D–D stretch (possibly obscured) but did indicate ν_s(MoD$_2$) at ~640 cm^{-1}. Mo(CO)(H$_2$)(dppe)$_2$ and our other group 6 H_2 complexes remain the only *isolable* H_2 complexes for which these bands have been observable (other than rare reports of ν(HH)[4,27]). Peaks due to lattice solvent appeared at 725 cm^{-1} for the toluene in Mo(CO)(H$_2$)(dppe)$_2$·2C$_7$H$_8$ and 672 cm^{-1} for benzene in Mo(CO)(H$_2$)(dppe)$_2$·3C$_6$H$_6$. As for M(CO)$_3$(PR$_3$)$_2$(H$_2$), a band near 600 cm^{-1}, probably due to ν(MoC) or δ(MoCO), shifts down ~15 cm^{-1} for the D_2 analogue, indicating mixing with a second, normally obscured δ(MoH$_2$) mode believed to lie in this region.[4]

For Mo(CO)(H$_2$)(dppe)$_2$, ν(CO) appeared at 1815 cm^{-1}, nearly 100 cm^{-1} higher than that for the agostic precursor (1723 cm^{-1}), consistent with sizable Mo→H_2 σ^* back-bonding. Increasing the electron-donating ability of the phosphine ligands by substituting Et for Ph leads to even greater population of H_2 σ^*, resulting in cleavage of the H_2 and formation of the *dihydride* MoH$_2$(CO)(Et$_2$PC$_2$H$_4$PEt$_2$)$_2$, characterized by X-ray diffraction[16] (Figure 2). ^{1}H NMR spectra of the latter and the *i*-Bu analogue showed classical quintet hydride resonances with J(PH) = 34 Hz, consistent with stereochemically nonrigid 7-coordinate structures. Below −25 °C, the signals broadened, and at the slow-exchange limit (−66 °C), an A_2BCX_2 pattern resulted (J(PH) = 23, 49, 64 Hz for R = Et),[16] consistent with the pentagonal bipyramidal structure observed in the X-ray structure. This behavior is very

(27) Harman, W. D.; Taube, H. *J. Am. Chem. Soc.* **1990**, *112*, 2261.

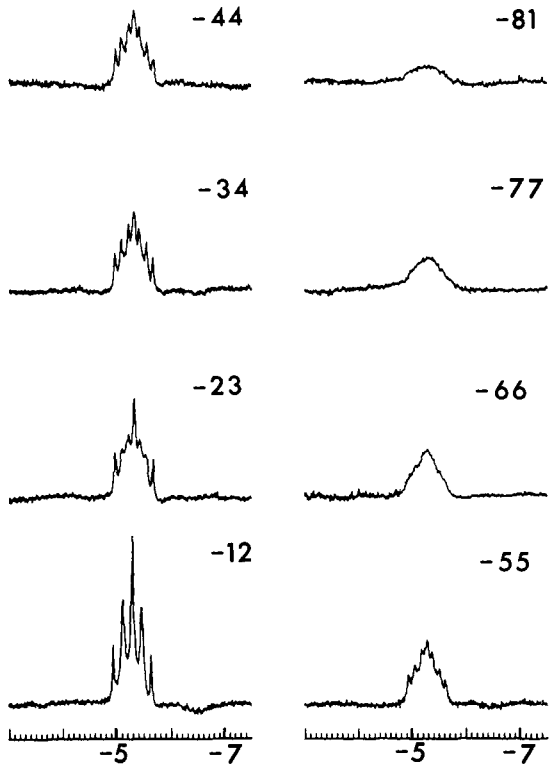

Figure 3. Variable-temperature ^1H NMR spectra (200 MHz, toluene-d_8) of $MoH_2(CO)(i\text{-}Bu_2PC_2H_4P\text{-}i\text{-}Bu_2)_2$.

similar to that for $CrH_2[P(OMe)_3]_5$, which has been shown by NMR to be fluxional and possess the same structure with distal hydrides in the pentagonal plane.[28] The *i*-Bu complex showed similar variable-temperature behavior, although the A_2BCX_2 pattern was reached at a higher temperature, −34 °C, and then collapsed to a broad singlet at −66 °C (Figure 3) for reasons that are as yet unclear. For both R = Et and R = *i*-Bu, no significant spectral differences were observed for the complexes prepared from HD, at either 25 or −90 °C. The T_1 was 370 ms at −70 °C and 1 s at 25 °C for R = Et and 200 ms for R = *i*-Bu (−70 °C), characteristic of hydride ligands.[1b] The lower value for the *i*-Bu species suggests the presence of some dihydrogen tautomer, which was also indicated by the lack of observation of a PHIP effect when para-H_2 was added to $Mo(CO)(i\text{-}Bu_2PC_2H_4P\text{-}i\text{-}Bu_2)_2$ to give the dihydride (tautomerization would destroy PHIP).

The spectrum of the Ph–Et species gave a broad unresolved multiplet signal near −4.3 ppm, possibly because of the inequivalent phosphorus atoms and isomeric interconversions expected in a fluxional system with an unsymmetrical diphosphine such as $Ph_2PC_2H_4PEt_2$. The signal did not change on HD substitution, which probably is not definitive here in light of the complex coupling situation.

IR bands were found for $MoH_2(CO)(depe)_2$ at 1647 cm^{-1} (medium) and ~720 cm^{-1} (weak, partially obscured), corresponding to ν(MoH) and δ(MoH), which shifted to 1194 and 528 cm^{-1} for the deuteride. These bands and hence the hydride structure were retained in solution (alkane solvents). The *i*-Bu and Ph–Et analogues showed similar ν(MoH) bands (Table III), indicating formulation as hydrides.

$H_2 + D_2 \rightarrow$ 2HD Isotopic Scrambling Catalyzed by $Mo(CO)(R_2PC_2H_4PR_2)_2$ and $Mo(CO)_3(PCy_3)_2$. Previous work showed that H_2/D_2 scrambling to give HD occurred over solid or solution phases of $W(CO)_3(PR_3)_2(H_2)$.[2b] H/D exchange with phosphine ligands does not occur in these systems, as confirmed by IR (ν(CD) bands were not seen in the complexes after exchange), and the scrambling mechanism remains an enigma. In order to determine if the molybdenum species also give exchange,

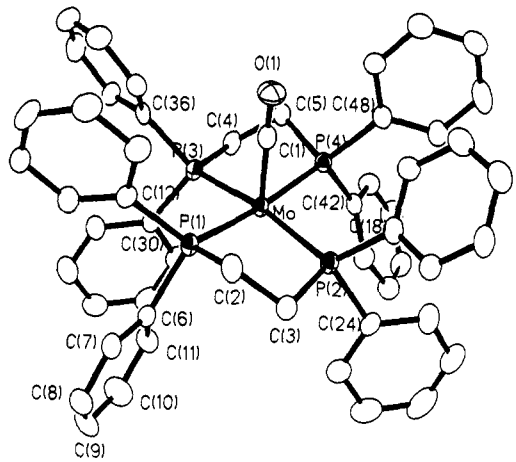

Figure 4. ORTEP drawing of the X-ray structure of $Mo(CO)(H_2)$-$(dppe\text{-}d_{20})_2\cdot 4.5C_6D_6$ with the atomic numbering scheme.

new gas–solid phase experiments were carried out by placing 1:1 H_2/D_2 mixtures (1 atm) over the following solid *precursor complexes* in closed flasks at ambient temperature: $Mo(CO)(R_2PC_2H_4PR_2)_2$ (R = Ph, Et) and $Mo(CO)_3(PCy_3)_2$. The molar ratios of total gas to complex were greater than 1 (up to 10 for the latter), i.e. *catalytic* scale, and the complexes and vessel were thoroughly vacuum-dried immediately before gas addition to avoid involvement of H_2O in the exchange. Mass spectral analyses showed that statistical scrambling (to 50% HD, 25% H_2, 25% D_2) for the Mo–H_2 complexes was complete within 9 d, although the exchange probably occurred in significantly less time. For R = Et, which forms a *dihydride*, the scrambling was only ~50% complete in this time, indicating that the presence of a labile H_2 ligand is a crucial factor (a small equilibrium amount of H_2 complex may account for the partial exchange). Interestingly, a sample of $[FeH(H_2)(dppe)_2][BF_4]$ (obtained from Morris[29]) served as a good "blank" because very little H_2/D_2 scrambling was seen over it after 9 d (<7% HD). This is probably because the H_2 ligand is nonlabile at 25 °C in this complex in the solid (H/D exchange does occur in solution[1d]).

Molecular Structure of $Mo(CO)(H_2)[(C_6D_5)_2PC_2H_4P(C_6D_5)_2]_2\cdot 4.5C_6D_6$. The deuterio phosphine complex was synthesized to reduce the background in the neutron diffraction experiment. The coordination geometry as determined from the single-crystal X-ray structural determination is quite similar to that previously described for the protio forms.[15] The complex adopts a pseudooctahedral geometry, with the dihydrogen ligand occupying the coordination site trans to the carbonyl group. An ORTEP drawing is shown in Figure 4. The Mo–C(1) (carbonyl) distance is 1.933 (5) Å, which is approximately equal to the value of 1.973 (16) Å found in the related dinitrogen complex $Mo(N_2)(CO)(dppe)_2$ and longer than the value of 1.903 (9) Å found in the unsaturated complex $Mo(CO)(dppe)_2$.[14] The molybdenum–phosphorus distances vary from 2.423 (1) to 2.447 (2) Å, with an averaged value of 2.438 (2) Å. The angles about the molybdenum in the plane of the phosphorus atoms are distorted by the smaller bite angle necessitated by the chelating phosphine ligands; the angles P(1)–Mo–P(2) and P(3)–Mo–P(4) are the most acute, at 80.6 (1) and 80.3 (1)°, respectively. There is a slight displacement of the molybdenum atom out of the plane formed by the four phosphorus atoms (0.0413 Å) toward the carbonyl unit. The diphosphine units are twisted, giving rise to two acute (P(1)–Mo–C(1) = 86.1 (1)°, P(4)–Mo–C(1) = 88.8 (1)°) and two obtuse (P(2)–Mo–C(1) = 91.6 (2), P(3)–Mo–C(1) = 97.5 (2)°) phosphorus–metal–carbon angles.

The complex $Mo(CO)(H_2)(dppe)_2$ crystallizes in one of a number of morphologies, depending on the degree of solvation. We have previously characterized a bis(toluene) solvate which crystallizes in a monoclinic morphology and a tris(benzene) solvate

(28) Van-Catledge, F. A.; Ittel, S. D.; Jesson, J. P. *Organometallics* **1985**, *4*, 18.

(29) The sample was the same as that used for inelastic neutron scattering in ref 13c.

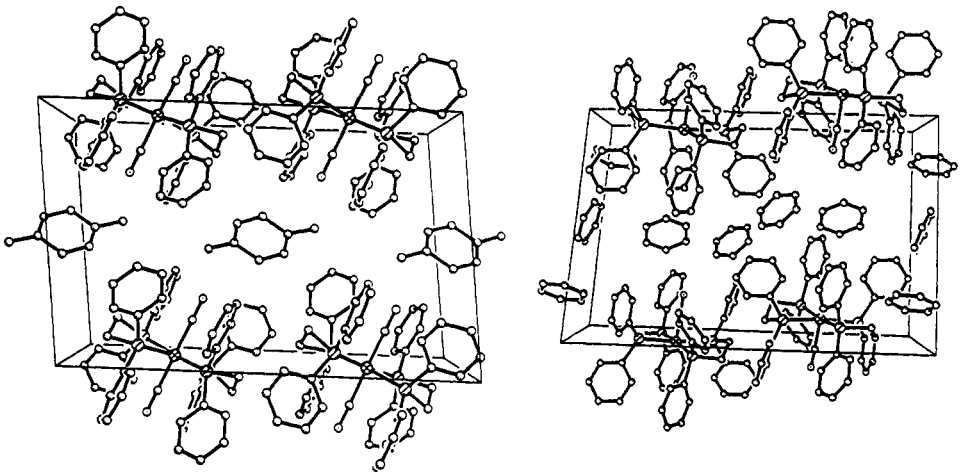

Figure 5. Packing diagrams of X-ray structures of (right) $Mo(CO)(H_2)(dppe\text{-}d_{20})_2\cdot 4.5C_6D_6$ in $P\bar{1}$ and (left) $Mo(CO)(H_2)(dppe)_2\cdot 2C_7H_8$ in $P2/c$ (showing 2-fold disorder).

which crystallizes in an orthorhombic space group.[15] The triclinic structure described herein occludes no fewer than 4.5 molecules of benzene per metal unit, although the crystals were grown under conditions similar to those for the latter (except possibly for solute concentration). The flexibility of the solvation state is due to the existence of channels which can accommodate a variable number of solvent molecules (Figure 5). The degree of solvation appears to have little effect on the structural parameters of the molybdenum unit, however, except for a slight perturbation in the relative twisting of the diphosphine units. In the heavily solvated triclinic structure, the dihedral angle formed by the P(1)–Mo–P(2) and P(3)–Mo–P(4) planes is 11.4°, while the comparable angle in the structure of the toluene solvate is 6.4°. This difference in geometry may be reflected in the barriers to hydrogen rotation in the two forms (vide infra). In both of the previously determined structures of the complex, the carbonyl and hydrogen ligands are disordered about a 2-fold symmetry axis. This complicates the mathematical model of the structure and limits the accuracy of any determination of the hydrogen positions. The triclinic structure is not complicated by this disorder, and so we chose to use this morphology for the neutron structural determination.

The coordination of the dihydrogen unit to the metal as determined by neutron diffraction is depicted in Figure 6. The complex does not undergo any significant structural changes between 233 and 12 K (see Table II). The hydrogen is bound symmetrically to the metal center, with an average Mo–H distance of 1.92 (1) Å and a metal–H_2(midpoint) distance of 1.886 Å. The former compares to the distance of 1.616 (10) Å found in the iron complex $[Fe(H_2)H(dppe)_2][BPh_4]$[3] and that of 1.89 (1) Å determined for the tungsten complex $W(CO)_3(P\text{-}i\text{-}Pr_3)_2(H_2)$.[2] The hydrogen molecule aligns itself along the P(1)–Mo–P(4) vector; the dihedral angles H(9)–H_2(midpoint)–Mo–P(1) and H(10)–H_2(midpoint)–Mo–P(4) are 15.5 and 12.6°, respectively. This eclipsed configuration is also found in the related iron complex.[3] The origin of this orientation will be discussed below. The hydrogen displays a high degree of librational motion, as evidenced by the large thermal ellipsoids elongated in the direction of H_2 rotation. This motion gives rise to an unusually large apparent bond shrinkage;[30] the refined distance H(9)–H(10) is 0.736 (10) Å, which is shorter than the value of 0.74 Å found in free H_2. We have attempted to apply a correction to this bond distance for the effects of thermal motion employing the program THMA11.[31] The librational motion was modeled about the axis from the midpoint of the hydrogen molecule to the molybdenum. Due to the lack of knowledge of the force constants for Mo–H_2 bonding, no attempt was made to subtract the internal vibrational motion of the hydrogen atoms; this limits the quality of the fit

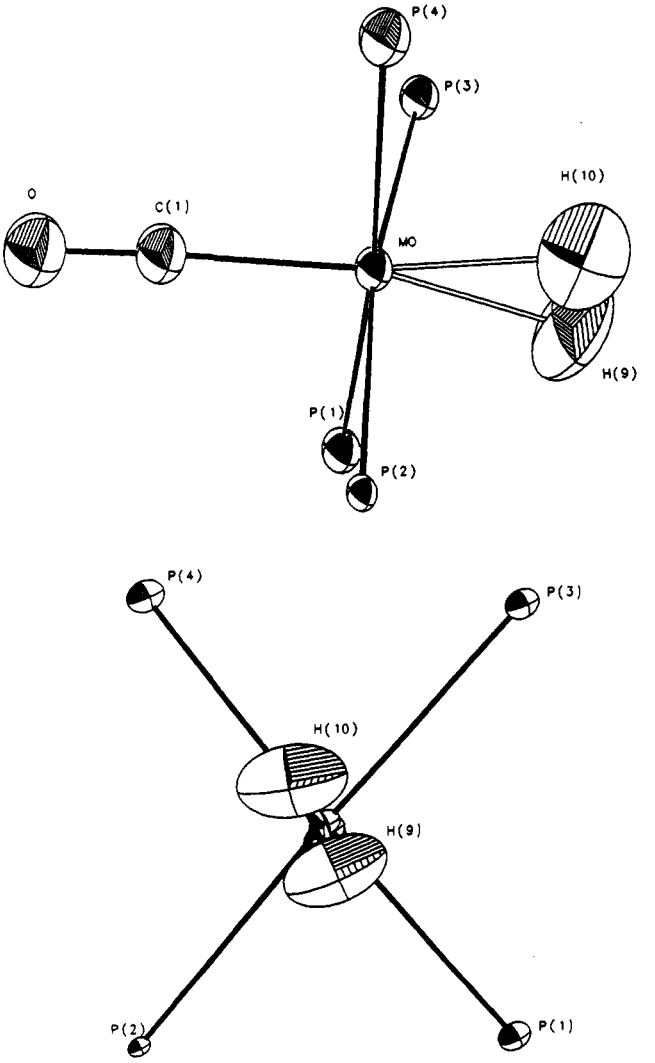

Figure 6. ORTEP drawings of two views of the metal coordination sphere of $Mo(CO)(H_2)(dppe\text{-}d_{20})_2\cdot 4.5C_6D_6$ (neutron).

to a rigid-body model with one internal degree of freedom and produces an overestimation of the correction to the bond length. The calculated corrected bond length lies in the range 0.85–0.88 Å. Assuming an overcorrection of 33–50%,[32] the "true" bond

(30) (a) Cruickshank, D. W. J. *Acta Crystallogr.* **1956**, *9*, 757. (b) Busing, W. R.; Levy, H. A. *Acta Crystallogr.* **1964**, *17*, 142.

(31) Maverick, E. F.; Trueblood, K. N. *THMA11-Program for Thermal Motion Analysis*; UCLA: Los Angeles, CA, 1988.

(32) The authors thank Profs. Maverick and Trueblood for their assistance and helpful suggestions regarding the magnitude of overcorrection of the thermal motion analysis.

length is postulated to lie in the range 0.80–0.85 Å. A somewhat longer length of 0.88 Å has been determined by solid-state ^{1}H NMR by Zilm on an unsolvated form of $Mo(CO)(H_2)(dppe)_2$.[6c] The NMR distance in $W(CO)_3(P\text{-}i\text{-}Pr_3)_2(H_2)$ (0.890 (6) Å) had previously been found to be 0.07 Å longer than the neutron distance.[33] However, NMR directly measures the H–H internuclear separation (rotational and other dynamics are not factors) and should be a more accurate and precise gauge than neutron diffraction.

Inelastic-Neutron-Scattering Studies of H_2 Rotation. We have investigated the hindered rotation of the dihydrogen ligand by inelastic neutron scattering (INS), using techniques and instrumentation as previously described.[4,13] These measurements allow a determination of the barrier to rotation of the dihydrogen ligand, which can be directly related to the strength of the back-bonding $d\pi(\text{metal}) \rightarrow \sigma^*(H_2)$. The reason for this is that the overlap of these orbitals does depend on the rotation angle of the dihydrogen around the M–H_2 axis, which gives this bond a directional property. Donation from the $\sigma(H_2)$ orbital, on the other hand, would be isotropic about this axis. Both of these interactions will weaken the H–H bond and strengthen the M–H bond, but only the back-bonding can lead to the actual cleavage of the H–H bond. The reason for this is that a three-center σ-bond is overall of bonding character. Other measures of the degree of H–H bond activation, such as the H–H distance and ν(HH), would on the other hand be sensitive to both of the above electronic interactions.

In order to derive a barrier height from measurements of the transitions of the hindered H_2 rotor, a model for this rotation has to be assumed. Because of the strong H–M interaction (relative to e.g. sorbed H_2), we have taken the rotation to be constrained to a plane perpendicular to the M–H_2 axis. Solid-state NMR measurements[6c] on related complexes have placed an upper limit on a possible librational amplitude out of this plane of about 6°. In addition, we have assumed that the rotation is subject to a simple double-minimum potential given by the crystallographically determined equilibrium orientation of the H_2 ligand. In some cases,[4,13c] a smaller 4-fold term needs to be added to the potential in order to achieve agreement with the measurements of the rotational transitions. We suspect that the reason for this is simply that the potential is in fact not exactly sinusoidal, so that the 4-fold term primarily changes the shape of the well rather than giving an indication of a second equilibrium orientation (90° away) of the H_2 at some higher energy. We cannot, however, rule out the latter possibility.

In most of our previous studies,[4,13] we have measured both the torsions (transition to the excited librational state) and the splitting of the librational ground state. The latter arises from the fact that the wave functions for the dihydrogen rotor in the two potential wells 180° apart overlap so that, because of the indistinguishability of the two protons, the ground state must split into two levels. This rotational tunnel splitting varies approximately exponentially with rotational barrier height and is therefore a very sensitive measure of the latter even without determination of the torsional transitions, provided a proven model is available for the system.

Measurements were therefore carried out on the splitting of the librational ground state by inelastic neutron scattering. The resulting spectrum (5 K) of the same sample of $Mo(CO)(H_2)(dppe\text{-}d_{20})_2\cdot 4.5C_6D_6$ used in the neutron diffraction structure is shown in Figure 7. The peaks observed on either side of the elastic peak correspond to the up (neutron energy loss) and down (energy gain) transitions within the librational ground state. The two sets of peaks (12.87 and 11.59 cm^{-1}, with the former having roughly twice the intensity of the latter) have similar structure; the doublet is partially resolved on the neutron energy loss side because the resolution of the spectrometer is better for energy loss than energy gain.

The origin of the doublet structure is likely to be some small amount of disorder in the molecular structure. A similar effect

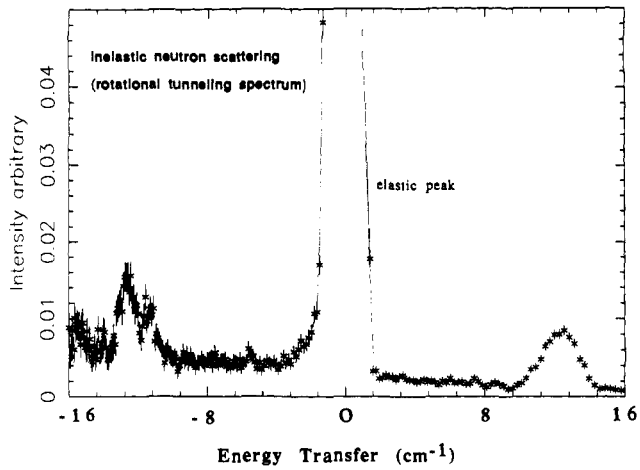

Figure 7. Rotational tunneling spectrum of $Mo(CO)(H_2)(dppe\text{-}d_{20})_2\cdot 4.5C_6D_6$ (T = 5 K).

was observed[13b] in the rotational tunneling spectrum of $W(CO)_3(H_2)(P\text{-}i\text{-}Pr_3)_2$, where structural disorder has been observed in the phosphine on one end of the complex. The way such a disorder could give rise to structure in the rotational tunneling lines is most likely through direct nonbonded interactions between the atoms on the phosphine and the dihydrogen. Thus, the two different orientations of the phosphine could slightly modulate the essentially electronic barrier to dihydrogen rotation. In the present case, however, no structural disorder was found within the limits of the crystal structure analysis (see above). Nonetheless, because of the extreme sensitivity of the rotational tunnel splitting to the barrier height, we are inclined to view the existence of some undetected disorder as much more likely than any of the other possible causes[13b] of such structure in the tunneling transitions.

With this information, we can derive a barrier height V_2 for dihydrogen rotation if the rotational constant of the H_2 ligand is known. This question does, however, present some difficulties, as the H–H bond is lengthened when coordinated, which reduces the rotational constant B from that of the free hydrogen molecule (59.3 cm^{-1}). While it may be assumed that the value of d(H–H) obtained from neutron diffraction studies would be most reliable, problems do occur because the analysis of the diffraction data frequently does not treat the dihydrogen ligand properly because of its very large librational amplitude (ca. ±20°). If the analysis is done in terms of standard thermal ellipsoids, these will create an artificially shortened H–H distance (see above). This problem is highlighted by the fact that the solid-state NMR studies[6c] consistently yield d(H–H) values that are substantially larger than those obtained by neutron diffraction. We have therefore, in the following analysis of the barrier height, used the range of values of d(H–H) obtained from the THMA correction procedure described above. For d(H–H) = 0.80 Å, this yields B = 50.7 cm^{-1} and a barrier height V_2 = 0.77 kcal/mol if we use the intensity-weighted mean rotational tunneling frequency of the tunneling spectrum (Figure 7) for the calculation. For a d(H–H) of 0.85 Å, the barrier would be 0.64 kcal/mol.

We have also collected INS data on the title complex crystallized with two toluene-d_8 solvate molecules instead of 4.5 benzene-d_6, using the cold neutron time-of-flight spectrometer MIBEMOL at the Orphee reactor of the Laboratoire Leon Brillouin. The rotational tunneling splitting was found to be 16.9 cm^{-1}, which gives a barrier of 0.5–0.6 kcal/mol depending on which of the above two values of d(H–H) is used to calculate B.

These are the lowest experimentally determined barriers to date in any dihydrogen complex and will be commented upon further in the Discussion.

Theoretical Analysis of the Structure of and Rotational Barrier of H_2 in $Mo(CO)(H_2)(dppe)_2$. The neutron diffraction structure of $Mo(CO)(H_2)(dppe)_2$ shows that the coordinated H_2 aligns preferably with the P(1)–Mo–P(4) direction. The structure is related to $[FeH(H_2)(dppe)_2]^+$, where the H_2 also aligns with one

(33) Zilm, K. W.; Merrill, R. A.; Kummer, M. W.; Kubas, G. J. *J. Am. Chem. Soc.* **1986**, *108*, 7837.

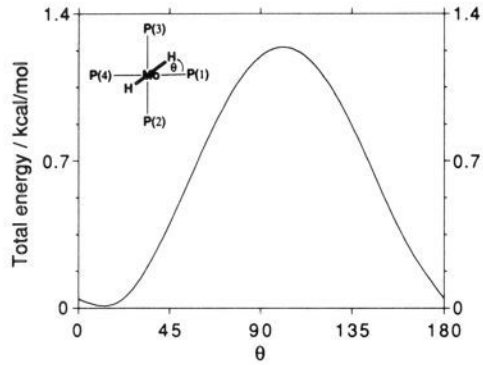

Figure 8. Total energy curve for $Mo(CO)(H_2)(PH_3)_4$.

of the P–Fe–P directions. This orientation in the iron complex was shown to be due to a hybridization of the d-orbitals available for back-bonding into $\sigma^*(H_2)$, which is caused by the distortion of the phosphines away from octahedral positions.[4] The distortion of the phosphines away from the site of H_2 causes a hybridization of the d-orbitals toward H_2 since this reduces the antibonding influence of the phosphines. Similarly, distortion of the phosphines toward H_2 will hybridize the d-orbital away from the site of H_2. The H_2 will preferentially align with a d-orbital which is the most hybridized toward it, since this increases metal–H_2 σ^* overlap and optimizes back-bonding (diagram **1**). In the Mo complex, P(1)

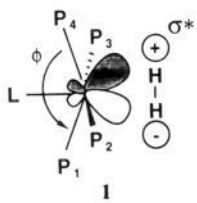

1

and P(4) are bent away from H_2 [P(1)–Mo–(H_2 midpoint) = 93.9°, P(4)–Mo–(H_2 midpoint) = 91.7°], with ϕ = 173.7 (2). The other two phosphines are bent toward H_2 [P(2)–Mo–(H_2 midpoint) = 86.0°, P(3)–Mo–(H_2 midpoint) = 85.0°]. Thus, we can already begin to rationalize the conformation found for H_2 along P(1)–Mo–P(4).

We have carried out extended Huckel calculations[34] on a model complex $Mo(CO)(H_2)(PH_3)_4$ using a structure directly related to the crystal structure of $Mo(CO)(H_2)(dppe\text{-}d_{20})_2 \cdot 4.5C_6D_6$. The *$H_2$ was rotated about the Mo–(H_2 midpoint) axis, and the variation* in total energy with the angle between the H–H and the Mo–P(1) directions, θ, was plotted (Figure 8; positive sign corresponds to counterclockwise rotation). We find a barrier to rotation of 1.2 kcal/mol with the energy minimum at θ = 11.0°. The calculated energy barrier is only 0.4 kcal/mol higher than that determined by neutron scattering, a satisfactory agreement. The actual position of H_2 is at θ = −15.5°, which may seem significantly different from 11.0°. However, in view of the large thermal anisotropies on the hydrogens *in the direction of the rotation*, we can consider this difference of 26.5° to be within experimental error.

The rotation of H_2 was recalculated using the entire structure of $Mo(CO)(H_2)(dppe)_2$, and a barrier of 1.4 kcal/mol with a minimum at θ = 6.2° was found. The similarity to that for $Mo(CO)(H_2)(PH_3)_4$ demonstrates that the latter is a good model for the actual complex. Examination of the entire structure shows that experimentally H_2 shows a tendency to reside in an area which has less steric influence from the phosphines (i.e. toward the CH_2CH_2 bridges between P(1) and P(2) rather than toward the phenyl rings lying between P(1) and P(3)). We can speculate that steric effects may play a minor role in fine-tuning the structure, but we cannot prove this by means of calculation.

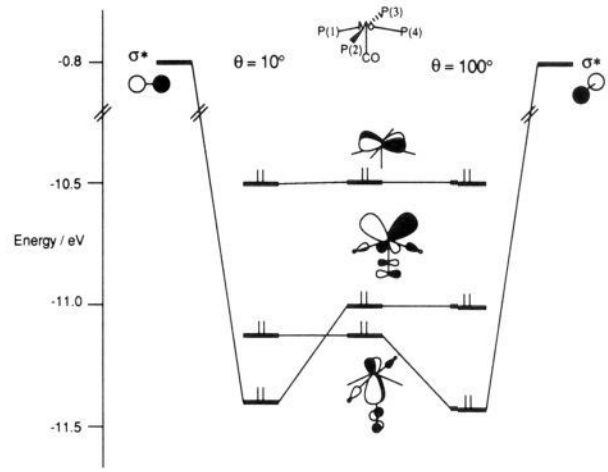

Figure 9. Interaction diagram for $Mo(CO)(PH_3)_4$ and H_2 at θ = 10° (total energy minimum) and θ = 100° (total energy maximum).

In order to carry out a more detailed examination of the structure and to support the bonding hypothesis outlined above, we have examined the bonding in the model complex by means of a fragment molecular orbital (FMO) calculation. Two neutral fragments were used, $Mo(CO)(PH_3)_4$ and H_2, and their interaction diagram is shown in Figure 9. The LUMO of the metal fragment is cylindrical and interacts with $\sigma(H_2)$, and since this interaction shows no variation upon H_2 rotation, it will not be considered further. The HOMO is the nonbonding d_{xy}-orbital of Mo. Below this orbital, there are the two possible candidates for back-bonding into $\sigma^*(H_2)$ presented by the metal fragment. The higher of these orbitals, derived from d_{xz}, is hybridized toward the vacant site as P(1) and P(4) bend away from it. This orbital is also hybridized away from stabilization by π^*(CO). The lower orbital, derived from d_{yz}, is hybridized away from the vacant site and toward the stabilizing influence of π^*(CO). Optimal back-bonding into $\sigma^*(H_2)$ is obtained when H_2 is aligned with d_{xz}, which wins in two ways over d_{yz}: it is both higher in energy (and thus closer to $\sigma^*(H_2)$) and overlaps better with $\sigma^*(H_2)$.

Discussion

H–H Bond Activation and Cleavage by $Mo(CO)(R_2PC_2H_4PR_2)_2$. The molybdenum system is ideally suited for demonstrating that *increasing the electron richness (i.e. raising the d-orbital energies)* of a metal center by inductive ligand effects leads to cleavage of bound H_2, ostensibly by overpopulating $\sigma^*(H_2)$. The results of variation of both phosphine size and basicity clearly show that electronic rather than steric factors dictate whether dihydrogen (R = Ph) or dihydride (R = Et, *i*-Bu, Ph–Et) complexes are formed. The bulkiness of the Ph and *i*-Bu diphosphines should be similar (PPh_3 and P-*i*-Bu_3 both have cone angles[35] near 145°), so it cannot be sterics that influence H–H rupture. Further confirmation that metal donation to H_2 σ^* controls H_2 cleavage is the fact that the tungsten analogue of the Mo–dihydrogen complex, $WH_2(CO)(Ph_2PC_2H_4PPh_2)_2$, has recently been found to be a *dihydride*,[36] tungsten being a better back-bonder than molybdenum.

The electronics of the metal center in Mo(CO)-(L)$(R_2PC_2H_4PR_2)_2$ can be evaluated by the positions of ν(NN) in the N_2 adducts. The frequencies (Table IV) decrease in the order Ph > Ph–Et > Et ~ *i*-Bu, corresponding to the expected increasing electron-richness of the metal center and activation of the N–N bond by back-donation. The positions of ν(NN) closely fit the correlation of Morris,[37] where H_2 complexes are predicted

(34) EHT calculations were carried out using the weighted H_{ij} formulation: Ammeter, J. H.; Burgi, H.-B.; Thibeault, J. C.; Hoffmann, R. *J. Am. Chem. Soc.* **1978**, *100*, 3686. The parameters for Mo were taken from: Summerville, R. H.; Hoffmann, R. *J. Am. Chem. Soc.* **1976**, *98*, 7240.

(35) Tolman, C. A. *Chem. Rev.* **1977**, *77*, 313.

(36) Ishida, T.; Mizobe, Y.; Tanase, T.; Hidai, M. *J. Organomet. Chem.* **1991**, *409*, 355.

(37) Morris, R. H.; Earl, K. A.; Luck, R. L.; Lazarowych, N. J.; Sella, A. *Inorg. Chem.* **1987**, *26*, 2674.

to be stable at metal centers which bind N_2 and give ν(NN) in the range 2060–2150 cm^{-1}. It is notable that ν(NN) for the Ph species (2090 cm^{-1}) is at the lower end of this range while the others are at or below the 2060-cm^{-1} borderline where hydrides are predicted. The Nujol mull values fit the correlation better than the solution-phase values, which are 20–30 cm^{-1} higher. Some of the properties of $MoH_2(CO)(R_2PC_2H_4PR_2)_2$ for R = alkyl are intermediate between those of dihydrogen and dihydride complexes, e.g. slight H_2 lability in solution. This might be suggestive of undetectable equilibrium amounts of the dihydrogen tautomer in the solution phase. ν(NN) for $W(CO)(N_2)(dppe)_2$ is reported to be 2030 and 2070 cm^{-1},[36] again correctly predicting the hydride formulation for $WH_2(CO)(dppe)_2$. Importantly, the relatively small shifts (~40 cm^{-1}) in ν(NN) with R show that the increase in electron flow to the metal caused by changing from phenyl to alkyl substituents (or Mo to W) is not severe, merely corresponding to "fine-tuning".

IR of solid products obtained from displacement of N_2 in $Mo(CO)(N_2)(R_2PC_2H_4PR_2)_2$ by SO_2 showed ν(SO) in positions (1164–1209 and 1038–1052 cm^{-1}) expected for planar M–η^1-SO_2 (corresponding to an electrophilic metal center capable of back-donation[38]). However, frequency correlations as above could not reliably be made because of uncertainties in structure/composition as indicated by ^{31}P NMR.

Despite the nearness of the H_2 in $Mo(CO)(H_2)(dppe)_2$ to cleavage, the corrected H–H neutron distance of 0.80–0.85 Å in the latter is surprisingly similar to the 0.82 Å values identically found in the neutron structures of $W(CO)_3(P\text{-}i\text{-}Pr_3)_2(H_2)$,[2] $FeH(H_2)(dppe)_2^+$,[3] and $FeH_2(H_2)(PPh_2Et)_3$.[4] Although the last three have not been corrected for H_2 libration, it is probable that their corrected distances will not significantly exceed 0.9 Å (the thermal ellipsoids for the Fe–dppe complex appear to be similar to those for the Mo complex, and the others are smaller). Despite the lack of precision caused by the H_2 motion, it is clear that none of the bond lengths are in the "long" range (>1 Å). This remarkable insensitivity to changes in metal/ligand/oxidation state suggests that *the reaction coordinate for H–H bond breaking shows relatively little change in H–H distance until bond rupture is quite imminent*, presumably when increased back-bonding can no longer be tolerated. Thus, the behavior might be likened more to the breaking of a taught rope than to the breaking of an elastic rubber band. Only a relatively small increase in back-bonding was needed for this to happen in the $MoH_2(CO)(R_2PC_2H_4PR_2)_2$ system, and apparently even finer tuning will be required to observe H–H lengthening or dihydrogen/dihydride equilibrium. By comparison, the well-studied systems of Morris, $MH(H_2)(R_2PC_2H_4PR_2)_2^+$ (M = Fe, Ru), did not cleave H_2 when R was varied exactly as in the Mo series,[3,39] indicating that the H_2 is further away from splitting. The presence of π-acceptor carbonyl ligands stabilizes dihydrogen coordination[40] and may well make the reaction coordinate less elastic for such complexes.

Another important consideration is the 2e three-center M–H_2 σ interaction, the principal bonding component. This interaction, like the M–H_2 σ^* back-bonding, also will weaken the H–H bond but cannot by itself break it since a three-center bond is overall of bonding character. It is possible that the lengthening of the H–H distance is not greatly affected by or is even offset by the extent of this σ-component, which could decrease as the electron richness of the complex increases.

Chemical properties also do not seem to be a valid indicator of H_2 activation; the hydrogen in the Mo–dppe complex is reversibly bound, but in the Fe–dppe cation, it is much less labile. The *hydridic* hydrogens in $MoH_2(CO)(Et_2PC_2H_4PEt_2)_2$ are actually more labile than the molecular hydrogen in the iron species (which is trans to a hydride, a high trans-effect ligand). This is opposite from the expected notion that tighter binding would correlate with a more activated or completely cleaved H_2. Furthermore, it should be noted that the coordination sphere of $MoH_2(CO)(depe)_2$ is completely different from that of $Mo(CO)(H_2)(dppe)_2$, with the hydrogens distal to each other in a pentagonal plane. In order for this dihydride to reversibly eliminate H_2 to form the presumably octahedral agostic species, structural rearrangement would first seem to be necessary. Ancillary ligand effects (trans influence, distortions from polydentate ligands), thermodynamic factors, and whether or not the precursor contains an agostic interaction probably are more important considerations in the reactivity of H_2 complexes than H–H bond length. Intramolecular C–H interactions clearly can facilitate H_2 dissociation by effectively "displacing" the H_2 and stabilizing the resulting unsaturated product (all the known group 6 congeners of $M(CO)_3(PR_3)_2$ and $M(CO)(P\text{–}P)_2$ have agostic interactions). The subtlety of dihydrogen versus dihydride binding can even extend to the nature of the counteranion in cationic species.[41]

Identifying the point at which H_2 cleaves and correlating this with spectroscopic/structural parameters are therefore difficult problems. Despite the fact that over 150 H_2 complexes are known, there are still insufficient data on the two most useful parameters, H–H distance and ν(HH), although with good reason. Crystallographic location of hydrogen is elusive, and ν(HH) not only is broad and weak but occurs in the worst possible region, near or within that for ν(CH). A further concern identified in this paper is the deleterious effect of H_2 rotation on H–H distance determination, even by low-temperature neutron diffraction. Complexes with symmetrical ligand sets should be avoided for structural study because of the likelihood of nearly free H_2 rotation and bond foreshortening effects. In regard to IR data as a measure of H–H bond activation, ν(HH) for $Mo(CO)(H_2)(dppe)_2$ is one of the lowest measured (2650 cm^{-1}), much lower than that for $Mo(CO)_3(PCy_3)_2(H_2)$ (estimated to be ~2950 cm^{-1} on the basis of ν(DD) observed at 2180 cm^{-1}) and lower than that for $W(CO)_3(PCy_3)_2(H_2)$ (2690 cm^{-1}). This reflects a more electron-rich metal center (only one electron-withdrawing CO versus three). The symmetric Mo–H_2 stretch (875 cm^{-1}) is ~10 cm^{-1} lower than that for $Mo(CO)_3(PCy_3)_2(H_2)$, whereas one might have expected it to be higher for a more activated H_2. However, this mode probably is more influenced by $H_2 \rightarrow M$ σ-donation, which would be lower for a less electrophilic metal center. Indeed, both $Cr(CO)_3(PCy_3)_2(H_2)$ and its W analogue show nearly identical values of 950 cm^{-1}, although the H_2 rotational barrier (hence back-bonding) for Cr was lower than that for W (1.3 vs 2.2 kcal/mol).[13e]

A large body of solution NMR data on H_2 complexes exists, and in certain well-defined series of complexes, good correlations of parameters such as J(HD) and T_1 with electronic factors and qualitative degrees of H_2 activation have been made. J(HD) in particular should be a reasonable measure of H–H distance, and values ranging widely from 4 to 34 Hz have been observed (primarily >28 Hz). Unfortunately, J(HD) could not be determined for the Re complexes with long H–H distances.[5,7] In most cases, the lower values (<28 Hz)[6d,39b,c,42] have been seen for strongly back-donating Os complexes where the H_2 is presumably nearly split (no crystallographic data). J(HD) < 27 Hz has not been reported for any group 6 or 7 or first-row complex and varied relatively little with R in $MH(H_2)(R_2PC_2H_4PR_2)_2^+$ for M = Fe,

(38) Ryan, R. R.; Kubas, G. J.; Moody, D. C.; Eller, P. G. *Struct. Bonding (Berlin)* **1981**, *46*, 47.

(39) (a) Morris, R. H.; Sawyer, J. F.; Shiralian, M.; Zubkowski, J. D. *J. Am. Chem. Soc.* **1985**, *107*, 5581. (b) Bautista, M.; Earl, K. A.; Morris, R. H.; Sella, A. *J. Am. Chem. Soc.* **1987**, *109*, 3780. (c) Bautista, M. T.; Earl, K. A.; Morris, R. H. *Inorg. Chem.* **1988**, *27*, 1124.

(40) (a) Hay, P. J. *J. Am. Chem. Soc.* **1987**, *109*, 705. (b) Lin, Z.; Hall, M. B. *J. Am. Chem. Soc.* **1992**, *114*, 6102.

(41) Bianchini, C.; Mealli, C.; Peruzzini, M.; Zanobini *J. Am. Chem. Soc.* **1992**, *114*, 5905.

(42) (a) Bautista, M. T.; Earl, K. A.; Maltby, P. A.; Morris, R. H. *J. Am. Chem. Soc.* **1988**, *110*, 4056. (b) Mezzetti, A.; Del Zotto, A.; Rigo, P.; Farnetti, E. *J. Chem. Soc., Dalton Trans.* **1991**, 1525. (c) Siedle, A. R.; Newmark, R. A.; Korba, G. A.; Pignolet, L. H.; Boyle, P. D. *Inorg. Chem.* **1988**, *27*, 1593. (d) Collman, J. P.; Wagenknecht, P. S.; Hembre, R. T.; Lewis, N. S. *J. Am. Chem. Soc.* **1990**, *112*, 1294. (e) Collman, J. P.; Hutchison, J. E.; Wagenknecht, P. S.; Lewis, N. S.; Lopez, M. A.; Guilard, R. *J. Am. Chem. Soc.* **1990**, *112*, 8206. (f) Harman, W. D.; Taube, H. *J. Am. Chem. Soc.* **1990**, *112*, 2261. (g) Li, Z.-W.; Taube, H. *J. Am. Chem. Soc.* **1991**, *113*, 8946. (h) Bianchini, C.; Mealli, C.; Peruzzini, M.; Zanobini, F. *J. Am. Chem. Soc.* **1987**, *109*, 5548. (i) Jia, G.; Morris, R. H. *J. Am. Chem. Soc.* **1991**, *113*, 875. (j) Chinn, M. S.; Heinekey, D. M. *J. Am. Chem. Soc.* **1990**, *112*, 5166.

Ru.[3,39] These data thus fit the supposition that most H_2 complexes can be expected to have "short" H–H bonds (<0.9 Å) unless the H_2 is very close to the point of splitting, coordinated to strongly back-bonding metal centers, or interacting with cis ligands. It is puzzling however that J(HD) is at the very high end, 34 Hz, and that the H–H distance is not longer for $Mo(CO)(H_2)(dppe)_2$, which would seem to have a highly activated H_2. The complex does not even show a dihydride tautomer in solution, although this may be due to the relatively large structural rearrangement needed.

Attempts to use the PHIP phenomenon[20] as a measure of H_2 activation or to differentiate between dihydrogen and dihydride products failed, presumably because even a small amount of reversibility in H–H bond breaking/forming destroys the polarization effect. Perhaps only completely classical hydrides such as $IrH_2Cl(CO)(PPh_3)_2$ will show this effect, but this remains to be tested.

Finally, H–H distances determined by solid-state NMR also failed to show significant variation with ligand sets and the central metal in the group 6 complexes. For example, $Mo(CO)(H_2)(dppe)_2$, $Mo(CO)_3(PCy_3)_2(H_2)$, and $W(CO)_3(PR_3)_2(H_2)$ (R = Cy, *i*-Pr) all gave similar values (0.87–0.89 Å).[13c,33] Distances >1 Å have been measured for $CpRuL_2(H_2)^+$ species, however, and further correlations of NMR and crystallographic parameters will be needed to assess the validity of either technique in defining the reaction coordinate for oxidative addition. Presumably, as H–H becomes longer, its rotational dynamics should decrease, and the bond lengths determined by these two methods should become more similar.

Rotational Barrier Heights and Theoretical Studies. Theoretical considerations suggest that the degree of distortion of the MP_4 skeleton is largely responsible for the ability of the complex to bind dihydrogen and for the degree of back-bonding from the metal d-orbital to H_2 σ^*, hence the barrier height for H_2 rotation. In $Mo(CO)(H_2)(dppe)_2$, the calculated barrier (1.39 kcal/mol) is approximately twice the measured values (0.5–0.8 kcal/mol). This is a degree of agreement similar to that for $FeH_2(H_2)(PEtPh_2)_3$, where the experimental and theoretical values were 1.1 and 2 kcal/mol.[4] We consider this agreement to be very satisfactory in view of the relatively simple level of the calculations. The equilibrium position of the dihydrogen ligand in these complexes is also fairly well accounted for by the electronic calculations. In both the Mo and Fe species, the potential minimum appears to be rather flat (the energy minimum was more than 25° away from the experimental position in the Mo complex). Steric effects, including even the influence of lattice solvent on distortions of the MoP_4 skeleton, thus may play a role in determining the actual equilibrium position within this flat potential and also rotational barrier heights. However, the calculations reproduce the actual minimum within experimental error, considering that the hydrogens in H_2 show a large thermal anisotropy in the direction of rotation and that the potential energy surface around this region must be rather flat.

The barriers for the two solvates of $Mo(CO)(H_2)(dppe)_2$ may also be compared with the larger value of 1.8 kcal/mol for the related complex $[FeH(H_2)(dppe)_2]BF_4$.[13c] In both the Mo- and Fe–dppe complexes, the H_2 ligand is roughly aligned with the P(1)–M–P(4) axis, wherein the phosphines are bent away from the dihydrogen ligand (diagram **1**). This distortion is largest for the iron complex, P(1)–M–P(4) (ϕ) = 163.0 (1)°,[39a] followed by those for $Mo(CO)(H_2)(dppe\text{-}d_{20})_2 \cdot 4.5C_6D_6$, 173.7 (2)°, and its toluene solvate,[15] 174.5 (1)°. Back-bonding is therefore expected to be more effective in the iron complex than in the molybdenum complex, resulting in a higher barrier to rotation, which is indeed observed. The dihedral angles between the planes formed by P(1)–Mo–P(2) and P(3)–Mo–P(4) are actually a better indicator of the degree of overall distortion of the MoP_4 skeleton than ϕ. The dihedral angles are 11.4° in the benzene solvate and only 5.7° in the toluene solvate, and the rotational barrier is correspondingly ~0.2 kcal/mol lower for the latter. These results illustrate how easily bidentate ligands can distort around the metal in d^6 ML_5 fragments (influenced even by crystal packing/solvation forces) and the sensitivity of the INS technique in measuring the effect on $M–H_2$ bonding.

In a recent, more sophisticated ab-initio calculation on several Fe complexes, Maseras et al.[43] do not give values for the barrier to dihydrogen rotation but do get reasonable agreement for the structural parameters of $FeH(H_2)(dppe)_2^+$. These authors also make the point that the degree to which the phosphines bend away from the dihydrogen ligand indicates how strongly the latter is bound to the metal, since the phosphines would bend toward the coordination site if it is empty.

Summary

The cleavage of H_2 to hydride when the basicity of the phosphines in $Mo(CO)(H_2)(R_2PC_2H_4PR_2)_2$ was increased fit perfectly with the bonding and activation models that implicate $M \rightarrow H_2$ σ^* back-bonding as crucial to H_2 splitting. However, several findings concerning the H–H bond length and the general question of the reaction coordinate for cleavage of H_2 were surprising and will require further exploration. The foreshortening effect of libration of the H_2 in $Mo(CO)(H_2)(dppe)_2$ on neutron determination of H–H bond length even at 12 K further complicates the problem of accurate hydrogen location. This effect correlated with the very low H_2 rotational barriers (0.5–1.0 kcal/mol) determined both experimentally and theoretically and expected for a complex with a binding site of nearly 4-fold symmetry. Techniques that are less sensitive to hydrogen motion such as solid-state NMR thus take on added importance for determination of H–H separations.

The statistical isotopic scrambling of H_2/D_2 to give HD over solid $Mo(CO)(H_2)(dppe)_2$ but not $MoH_2(CO)(depe)_2$ was important for several reasons, foremost being the demonstration that the presence of labile η^2-H_2 is crucial to facile exchange. The fact that the *catalytic*-scale system contained little if any adventitious H_2O indicated that scrambling mechanisms based on intermediacy of H_2O (e.g. deprotonation of η^2-H_2) are not likely.[44] Determination of the actual pathway remains a challenge.

Unexpectedly, $Mo(CO)(H_2)(dppe)_2$ showed neither an elongated H–H bond length nor equilibrium with a dihydride tautomer despite the apparent nearness of the H_2 to cleavage. It is now the fourth dihydrogen complex to show a neutron-determined H–H distance of ca. 0.82 Å despite widely varying ligand sets, central metals, and charges. It thus appears that the reaction coordinate for oxidative addition of H_2 may be rather flat until relatively precipitous cleavage of the H_2. Relative stabilities/structures of the dihydride product may be an important factor in the reaction coordinate, but to what extent is still uncertain. Although some evidence has appeared for rhenium–dihydrogen complexes with longer H–H separations, it is still not definitive.[45] In the Mo–diphosphine system, it is clear that complexes containing phosphines with basicities intermediate to those of dppe and depe will need to be prepared in order to observe bond lengthening and pinpoint H_2 splitting. Preliminary experiments indicate that H_2 complexes with significantly lower J(HD) (ca. 26 Hz) can be prepared, suggestive of increased H–H activation.

Acknowledgment. The authors thank Lori Van Der Sluys for preparation of dppe-d_{20}, Janet Nelson for ^{31}P NMR spectroscopy, and also R. White and G. Coddens for assistance with the inelastic neutron studies at the Institut Laue-Langevin, Grenoble, France, and the Laboratoire Leon Brillouin, Saclay, France, respectively. This work was funded initially by the U.S. Department of Energy, Division of Chemical Sciences, Office of Basic Energy Sciences, with subsequent support from Laboratory Directed Research and

(43) Maseras, F.; Duran, M.; Lledos, A.; Bertran, J. *J. Am. Chem. Soc.* **1991**, *113*, 2879.

(44) See also: Kubas, G. J.; Burns, C. J.; Khalsa, G. R. K.; Van Der Sluys, L. S.; Kiss, G.; Hoff, C. D. *Organometallics* **1992**, *11*, 3390.

(45) **Note Added in Proof**: It has come to our attention that neutron data supporting an elongated H–H distance near 1.1 Å has been obtained for a non-rhenium complex containing a cis hydride. It thus appears that a near continuum of H–H distances will be found in metal-coordination spheres.

Development funds for the neutron studies. This work has also benefited from the use of facilities at the Los Alamos Neutron Scattering Center, a national user facility funded as such by the Department of Energy, Office of Basic Energy Sciences.

Supplementary Material Available: Tables of fractional coordinates, general displacement parameter expressions (U's), and complete bond distances and angles (21 pages). Ordering information is given on any current masthead page.

Metal Dependence of the Nonplanar Distortion of Octaalkyltetraphenylporphyrins

L. D. Sparks,[†,‡] C. J. Medforth,[§] M.-S. Park,[‡] J. R. Chamberlain,[†] M. R. Ondrias,[‡] M. O. Senge,[§] K. M. Smith,[*,§] and J. A. Shelnutt[*,†,‡]

Contribution from the Fuel Science Department 6211, Sandia National Laboratories, Albuquerque, New Mexico 87185, Department of Chemistry, University of New Mexico, Albuquerque, New Mexico 87131, and Department of Chemistry, University of California, Davis, California 95616. *Received May 29, 1992. Revised Manuscript Received September 30, 1992*

Abstract: The biological activity of porphyrins and related tetrapyrroles in proteins may be modulated by nonplanar conformational distortions; consequently, two aspects of nonplanarity have been investigated in the highly nonplanar octaalkyltetraphenylporphyrins (OATPPs). In the first part, the effect of the central metal ion (M = Ni(II), Co(II), Cu(II), Zn(II), Co(III), Fe(III)) on the conformation of the OATPP macrocycle has been determined. Crystallographic studies reveal that the sterically encumbered, nonplanar porphyrin 2,3,7,8,12,13,17,18-octaethyl-5,10,15,20-tetraphenylporphyrin (OETPP) remains sufficiently flexible to show a small decrease in nonplanarity for large metal ions. This decrease in nonplanarity for the OETPP metal complexes is predicted by using a molecular mechanics force field derived from structural and vibrational data for planar metalloporphyrins. A detailed analysis of the crystal structures of the Co(II) and Cu(II) complexes of OETPP reveals that the metal-dependent changes in bond lengths and bond angles are qualitatively similar to the changes observed for the OEP complexes. As the metal size increases, both OEPs and OETPPs exhibit expansion of the meso bridges (increases in the C_α–C_m bond length and the C_α–C_m–C_α bond angle) and a movement of the coordinating nitrogen atoms away from the metal atom (increases in the M–N bond length and the C_α–N–C_α bond angle and a decrease in the N–C_α bond length). Furthermore, the frequencies of several structure-sensitive Raman lines correlate with structural parameters obtained from these crystallographic studies. In the second part, a combination of molecular mechanics and INDO/CI molecular orbital calculations successfully predicts the optical spectra of a series of highly substituted OATPPs with increasing nonplanar distortion. The success of these calculations indicates the importance of including both the macrocycle conformation and the peripheral substituents in the INDO calculations.

Introduction

Interest has recently been expressed in the role of nonplanar conformational distortions in modifying the biological properties of tetrapyrroles in the photosynthetic reaction center of *Rhodopseudomonas viridis*,[1] the photosynthetic antenna system of *Prosthecochloris aestuarii*,[2] methylreductase,[3] vitamin B_{12} and B_{12}-dependent enzymes,[4] and heme proteins.[5] In this regard, some octaalkyltetraphenylporphyrins (OATPPs) (Figure 1), which are nonplanar as a result of steric crowding of the peripheral substituents, have been used as model compounds to investigate the consequences of nonplanar conformational distortions.[6-14] Also, we are interested in using these highly substituted OATPPs to tailor biomimetic catalysts with a specified function and catalytic selectivity. For example, Fe, Mn, and Ru porphyrins catalyze the oxidation of alkanes,[15-18] mimicking the function of cytochrome P_{450}. The activity of these biomimetic porphyrin catalysts is determined primarily by the choice of metal, axial ligands, the electronic properties of the porphyrin macrocycle, and steric factors such as the incorporation of a substrate binding cavity.[19]

It is our goal to design substrate binding cavities for highly substituted porphyrins by using molecular modeling methods to select suitable substituents. A carefully designed binding cavity offers several benefits, including (1) the controlled access of various molecules to the active catalytic metal center, (2) enhanced binding affinity of the porphyrin for the substrate molecule of interest, (3) the trapping of intermediates of the reaction in the cavity for recombination, and (4) the prevention of undesired side reactions and catalyst self-destruction. Catalytic function may then be fine

* To whom correspondence should be addressed.
† Sandia National Laboratories.
‡ University of New Mexico.
§ University of California.

(1) (a) Deisenhofer, J.; Michel, H. *Angew. Chem., Int. Ed. Engl.* **1989**, *28*, 829-847. (b) Deisenhofer, J.; Michel, H. *Science* **1989**, *245*, 1463-1473.
(2) Tronrud, D. E.; Schmid, M. F.; Matthews, B. W. *J. Mol. Biol.* **1986**, *188*, 443-454.
(3) (a) Furenlid, L. R.; Renner, M. W.; Smith, K. M.; Fajer, J. *J. Am. Chem. Soc.* **1990**, *112*, 1634-1635. (b) Furenlid, L. R.; Renner, M. W.; Fajer, J. *J. Am. Chem. Soc.* **1990**, *112*, 8987-8989.
(4) Geno, M. K.; Halpern, J. *J. Am. Chem. Soc.* **1987**, *109*, 1238-1240.
(5) Alden, R. G.; Ondrias, M. R.; Shelnutt, J. A. *J. Am. Chem. Soc.* **1990**, *112*, 691-697.
(6) Barkigia, K. M.; Chantranupong, L.; Smith, K. M.; Fajer, J. *J. Am. Chem. Soc.* **1988**, *110*, 7566-7567.
(7) Barkigia, K. M.; Berber, M. D.; Fajer, J.; Medforth, C. J.; Renner, M. W.; Smith, K. M. *J. Am. Chem. Soc.* **1990**, *112*, 8851-8857.
(8) Renner, M. W.; Cheng, R.-J.; Chang, C. K.; Fajer, J. *J. Phys. Chem.* **1990**, *94*, 8508-8511.
(9) Medforth, C. J.; Berber, M. D.; Smith, K. M.; Shelnutt, J. A. *Tetrahedron Lett.* **1990**, *31*, 3719-3722.
(10) Shelnutt, J. A.; Medforth, C. J.; Berber, M. D.; Barkigia, K. M.; Smith, K. M. *J. Am. Chem. Soc.* **1991**, *113*, 4077-4087. The functional form used for the inversion energy was stated to be quadratic in the distortion angle, ω. Actually, a $1 - \cos\omega$ functional form was employed. The force constant for Ni inversion is zero and not 35 given in the original reference.
(11) Medforth, C. J.; Smith, K. M. *Tetrahedron Lett.* **1990**, *31*, 5583-5586.
(12) The nickel complex of porphyrin **4** could not be crystallized due to its poor solubility. The nickel complex of porphyrin **7** crystallizes in two conformations which are more akin to the crystal structure of tetragonal NiOEP ((a) Meyer, E. F. *Acta Crystallogr.* **1972**, *B28*, 2162-2167. (b) Cullen, D. L.; Meyer, E. F., Jr. *J. Am. Chem. Soc.* **1974**, *96*, 2095-2102) rather than the very nonplanar saddle conformations seen for the other nickel OATPPs. The copper complex of porphyrin **8** is essentially planar (Senge, M. O.; Medforth, C. J.; Sparks, L. D.; Shelnutt, J. A.; Smith, K. M. *Inorg. Chem.*, submitted).

0002-7863/93/1515-581$04.00/0